

AD-A135 849

EXACT AND FINITE-ELEMENT ANALYSIS OF LAMINATED SHELLS
(U) VIRGINIA POLYTECHNIC INST AND STATE UNIV BLACKSBURG
COLL OF ENGINEERING J N REDDY NOV 83 VPI-E-83-45

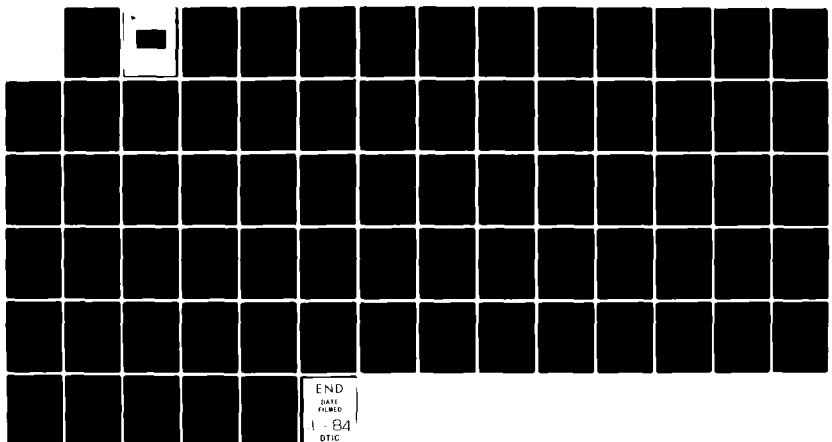
1/1

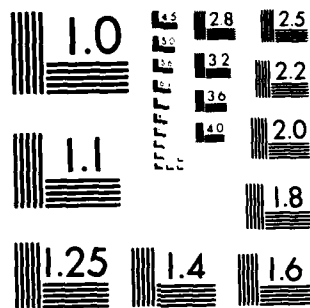
UNCLASSIFIED

AFOSR-81-0142

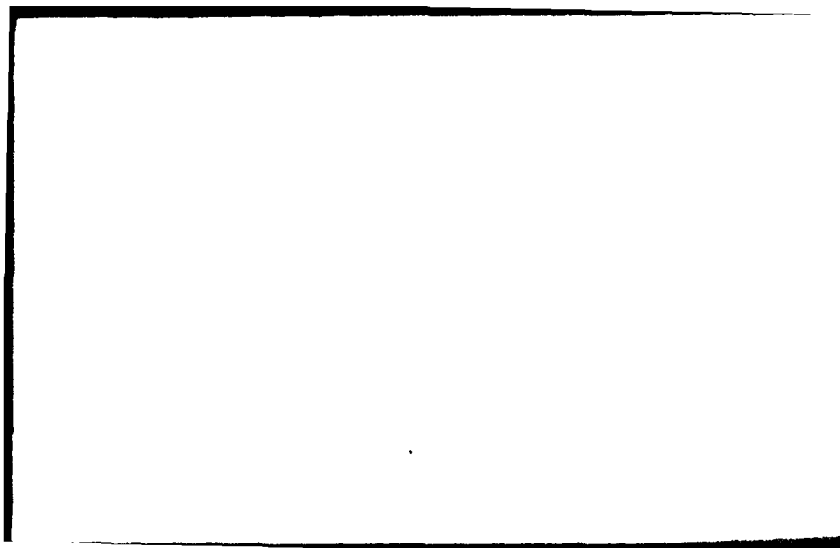
F/G 12/1

NL





MICROCOPY RESOLUTION TEST CHART
NATIONAL BUREAU OF STANDARDS-1963-A



The United States Air Force
AIR FORCE OFFICE OF SCIENTIFIC RESEARCH
Structural Mechanics Program
Bolling AFB, D. C. 20332

Grant No. AFOSR-81-0142-B
Technical Report No. AFOSR-81-5

Report VPI-E-83.45

EXACT AND FINITE-ELEMENT ANALYSIS OF LAMINATED SHELLS

J. N. Reddy

Department of Engineering Science and Mechanics
Virginia Polytechnic Institute and State University
Blacksburg, VA 24061

November 1983

This document has been approved
for public release and its use is
distributed as indicated.

DTIC

DEC 15 1983

A

Approved for	
GRANT	<input checked="" type="checkbox"/>
REPORT	<input checked="" type="checkbox"/>
Abstract	<input checked="" type="checkbox"/>
Summary	<input checked="" type="checkbox"/>
Availability Codes	
AVB	
AVC	
AVD	
AVE	
AVF	
AVG	
AVH	
AVI	
AVJ	
AVK	
AVL	
AVM	
AVN	
AVO	
AVP	
AVQ	
AVR	
AVS	
AVT	
AVU	
AVV	
AVW	
AVX	
AVY	
AVZ	

DTIC
COPY
INSPECTED
3

EXACT SOLUTIONS OF MODERATELY THICK LAMINATED SHELLS

By J. N. Reddy,¹ M. ASCEABSTRACT:

The paper contains an extension of Sanders shell theory for doubly-curved shells to a shear deformation theory of laminated shells. The theory accounts for transverse shear strains and rotation about the normal to the shell mid-surface. Exact solutions of the equations are presented for simply supported, doubly-curved, cross-ply laminated shells under sinusoidal, uniformly distributed, and concentrated point load at the center. Fundamental frequencies of cross-ply laminated shells are also presented. The exact solutions presented herein for laminated composite shells should serve as bench mark solutions for future comparisons.

INTRODUCTION

There exist a number of theories for layered anisotropic shells. Many of these theories were developed originally for thin shells, and are based on the Kirchhoff-Love kinematic hypothesis that plane sections normal to the undeformed midsurface remain plane and normal to the middle surface after deformation and undergo no thickness stretching. Surveys of various shell theories can be found in the works of Naghdi [16] and Bert [3,4], and a detailed study of thin ordinary (i.e., not laminated) shells can be found in the monographs by Kraus [14], Ambartsumyan [1], and Vlasov [20].

¹Professor of Engineering Science and Mechanics, Virginia Polytechnic Institute and State University, Blacksburg, VA 24061

The first analysis that incorporated the bending-stretching coupling (due to unsymmetric lamination in composites) is due to Ambartsumyan [2]. In his analyses Ambartsumyan assumed that the individual orthotropic layers were oriented such that the principal axes of material symmetry coincided with the principal coordinates of the shell reference surface. Thus, Ambartsumyan's work dealt with what is now known as laminated orthotropic shells rather than laminated anisotropic shells; in laminated anisotropic shells the individual layers are, in general, anisotropic and the principal axes of material symmetry of the individual layers coincide with only one of the principal coordinates of the shell (the thickness normal coordinate).

Dong, Pister, and Taylor [9] formulated a theory of thin shells laminated of anisotropic material that is an extension of the theory developed by Stavsky [9] for laminated anisotropic plates to Donnell's shallow shell theory (see Donnell [10]). Cheng and Ho [8] presented an analysis of laminated anisotropic cylindrical shells using Flügge's shell theory (see Flügge [12]). A first approximation theory for the unsymmetric deformation of non-homogeneous, anisotropic, elastic cylindrical shells was derived by Widera and his colleagues [25,26] by means of the asymptotic integration of the elasticity equations. For a homogeneous, isotropic material, the theory reduces to Donnell's equations.

All of the works reviewed above are based on Kirchhoff-Love's hypotheses in which the transverse shear deformation is neglected. These theories, known as the Love's first-approximation theories (see Love [15]) are expected to yield sufficiently accurate results when (i) the lateral dimension-to-thickness ratio is large; (ii) the dynamic excitations are within the low-frequency range; and (iii) the material anisotropy is not severe. However, application

of such theories to layered anisotropic composite shells could lead to as much as 30% or more errors in deflections, stresses, and frequencies.

The effects of transverse shear deformation and transverse isotropy, as well as thermal expansion through the thickness of cylindrical shells were considered by Gulati and Essenberg [12] and Zukas and Vinson [29]. Whitney and Sun [23,24] developed a shear deformation theory for laminated cylindrical shells that includes both transverse shear deformation and transverse normal strain as well as expansional strains.

Recently, Bert and his colleagues [6,7,13] presented exact solutions for bending and vibration of two-layer, cross-ply, thin cylindrical shells. These solutions are limited to cylindrical shells and sinusoidal distribution of the transverse load, and the procedure used is one similar to that used by Whitney and Leissa [21], Whitney and Pagano [22], Bert and Chen [5], and Reddy and Chao [17] for laminated composite plates. The present study is concerned with the development of exact solutions for simply supported, doubly-curved, cross-ply laminated shells. It is shown that, unlike plates, antisymmetric angle-ply laminated shells with simply supported boundary conditions do not admit exact solutions. Numerical results for transverse deflection and fundamental frequencies are presented for various cross-ply laminated shells.

DERIVATION OF EQUATIONS

Figure 1a contains a differential element of a doubly-curved shell. Here (ξ_1, ξ_2, ζ) denote the orthogonal curvilinear coordinates (shell coordinates) such that the ξ_1 - and ξ_2 - curves are lines of curvature on the midsurface $\zeta=0$, and ζ - curves are straight lines perpendicular to the surface $\zeta=0$. For the doubly-curved shells discussed here, the lines of principal curvature

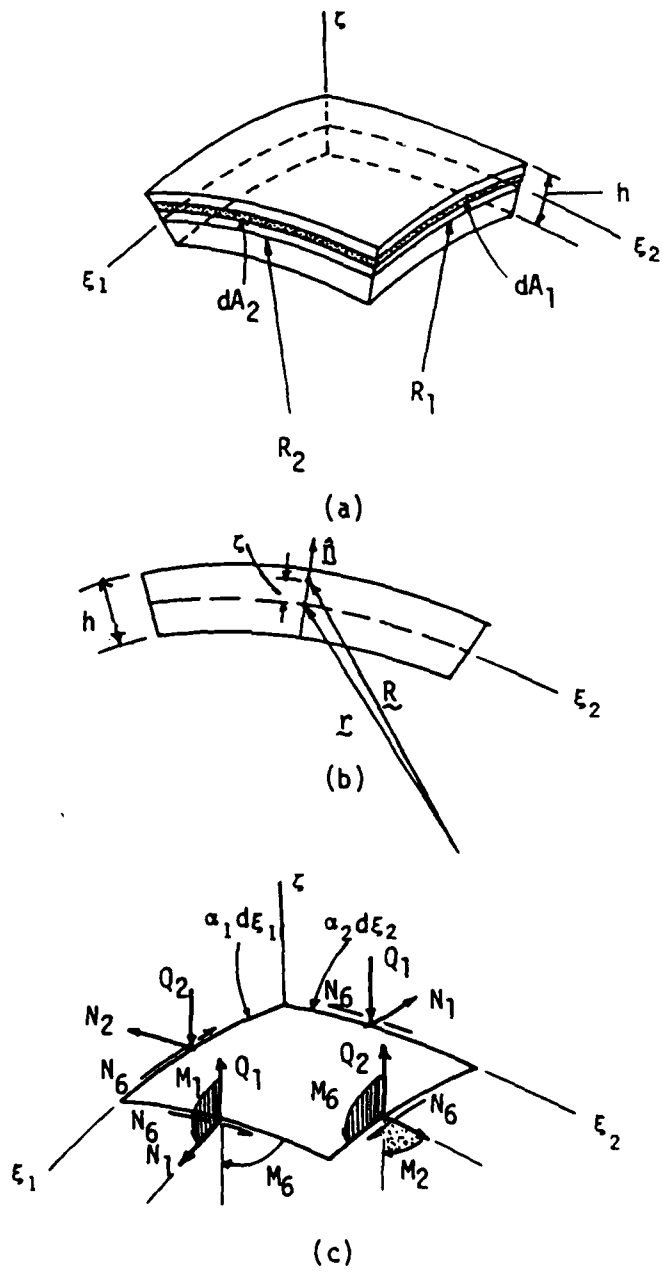


Figure 1. Geometry and stress resultants of a shell

coincide with the coordinate lines. The values of the principal radii of curvature of the middle surface are denoted by R_1 and R_2 .

The position vector of a point on the middle surface is denoted by \underline{r} , and the position of a point at distance ζ from the middle surface is denoted by \underline{R} (see Fig. 1b). The distance ds between points $(\xi_1, \xi_2, 0)$ and $(\xi_1 + d\xi_1, \xi_2 + d\xi_2, 0)$ is determined by

$$\begin{aligned} (ds)^2 &= d\underline{r} \cdot d\underline{r} \\ &= \alpha_1^2 (d\xi_1)^2 + \alpha_2^2 (d\xi_2)^2 \end{aligned} \quad (1)$$

where $d\underline{r} = \underline{r}_1 d\xi_1 + \underline{r}_2 d\xi_2$, the vectors \underline{r}_1 and \underline{r}_2 ($\underline{r}_i = \frac{\partial \underline{r}}{\partial \xi_i}$) are tangent to the ξ_1 and ξ_2 coordinate lines, and α_1 and α_2 are the surface metrics

$$\alpha_1^2 = \underline{r}_1 \cdot \underline{r}_1, \quad \alpha_2^2 = \underline{r}_2 \cdot \underline{r}_2. \quad (2)$$

The distance dS between points (ξ_1, ξ_2, ζ) and $(\xi_1 + d\xi_1, \xi_2 + d\xi_2, \zeta + d\zeta)$ is given by

$$\begin{aligned} (dS)^2 &= d\underline{R} \cdot d\underline{R} \\ &= L_1^2 (d\xi_1)^2 + L_2^2 (d\xi_2)^2 + L_3^2 (d\zeta)^2 \end{aligned} \quad (3)$$

where $d\underline{R} = \frac{\partial \underline{R}}{\partial \xi_1} d\xi_1 + \frac{\partial \underline{R}}{\partial \xi_2} d\xi_2 + \frac{\partial \underline{R}}{\partial \zeta} d\zeta$, and L_1 , L_2 , and L_3 are the Lame' coefficients

$$L_1 = \alpha_1 \left(1 + \frac{\zeta}{R_1}\right), \quad L_2 = \alpha_2 \left(1 + \frac{\zeta}{R_2}\right), \quad L_3 = 1 \quad (4)$$

It should be noted that the vectors $\frac{\partial \underline{R}}{\partial \xi_1}$ and $\frac{\partial \underline{R}}{\partial \xi_2}$ are parallel to the vectors $\frac{\partial \underline{r}}{\partial \xi_1} = \underline{r}_1$ and $\frac{\partial \underline{r}}{\partial \xi_2} = \underline{r}_2$.

From Fig. 1a, the elements of area of the cross sections are

$$\begin{aligned} dA_1 &= L_1 d\xi_1 d\zeta = \alpha_1 \left(1 + \frac{\zeta}{R_1}\right) d\xi_1 d\zeta \\ dA_2 &= L_2 d\xi_2 d\zeta = \alpha_2 \left(1 + \frac{\zeta}{R_2}\right) d\xi_2 d\zeta \end{aligned} \quad (5)$$

Let N_1 be the tensile force, measured per unit length along a ξ_2 - coordinate line, on a cross section perpendicular to a ξ_1 - coordinate line. Then the total tensile force on the differential element in the ξ_1 -direction is $N_1 \alpha_2 d\xi_2$. This force is equal to the integral of $\sigma_1 dA_2$ over the thickness,

$$N_1 \alpha_2 d\xi_2 = \int_{-h/2}^{h/2} \sigma_1 dA_2 d\zeta \quad (6)$$

where h is the thickness of the shell ($\zeta = -h/2$ and $\zeta = h/2$ denote the bottom and top surfaces of the shell). Using Eq. (5), we can write

$$N_1 = \int_{-h/2}^{h/2} \sigma_1 \left(1 + \frac{\zeta}{R_2}\right) d\zeta \quad (7)$$

Similarly, the remaining stress resultants per unit length can be derived.

The complete set is given by (see Fig. 1c).

$$\begin{Bmatrix} N_1 \\ N_2 \\ N_{12} \\ N_{21} \\ Q_1 \\ Q_2 \end{Bmatrix} = \int_{-h/2}^{h/2} \begin{Bmatrix} \sigma_1 \left(1 + \frac{\zeta}{R_2}\right) \\ \sigma_2 \left(1 + \frac{\zeta}{R_1}\right) \\ \sigma_6 \left(1 + \frac{\zeta}{R_2}\right) \\ \sigma_6 \left(1 + \frac{\zeta}{R_1}\right) \\ \sigma_5 \left(1 + \frac{\zeta}{R_2}\right) \\ \sigma_4 \left(1 + \frac{\zeta}{R_1}\right) \end{Bmatrix} d\zeta \quad (8)$$

$$\begin{pmatrix} M_1 \\ M_2 \\ M_{12} \\ M_{21} \end{pmatrix} = \begin{pmatrix} \zeta \alpha_1 (1 + \zeta/R_2) \\ \zeta \alpha_2 (1 + \zeta/R_1) \\ \zeta \alpha_6 (1 + \zeta/R_2) \\ \zeta \alpha_6 (1 + \zeta/R_1) \end{pmatrix}$$

Note that, in contrast to the plate theory (which is obtained by setting $1/R_1 = 1/R_2 = 0$), the shear stress resultants N_{12} and M_{21} , and twisting moments M_{12} and M_{21} are, in general, not equal. For shallow shells, however, one can neglect ζ/R_1 and ζ/R_2 in comparison with unity. Under this assumption, one has N_{12} and $N_{21} \equiv N_6$ and M_{12} and $M_{21} \equiv M_6$ (of course, for spherical shells we always have $N_{12} = N_{21}$ and $M_{12} = M_{21}$).

A set of simplifying assumptions that provides a reasonable description of the behavior of thin elastic shells is used to derive the equilibrium equations that are consistent, via virtual work, with the assumed displacement field:

1. the thickness of the shell is small compared to the principal radii of curvature ($h/R_1, h/R_2 \ll 1$);
2. the transverse normal stress is negligible;
3. normals to the reference surface of the shell before deformation remain straight but not necessarily normal after deformation (a relaxed Kirchhoff-Love's hypothesis);
4. The deflections are small compared with the shell thickness.

The shell under consideration is composed of a finite number of orthotropic layers of uniform thickness, as shown in Fig. 2. In view of assumption 1, the stress resultants in Eq. (8) can be expressed as

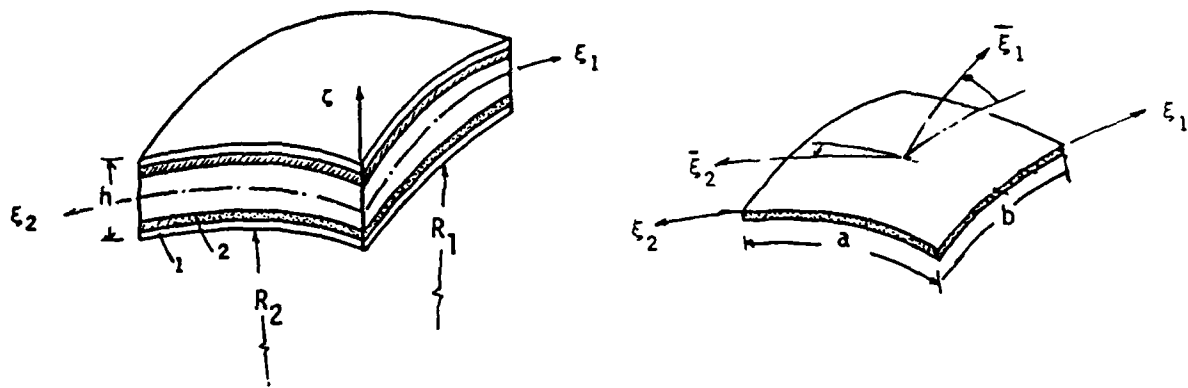


Figure 2. Laminated shell geometry and lamina details

$$(N_i, M_i) = \sum_{k=1}^N \int_{\zeta_{k-1}}^{\zeta_k} \alpha_i(1, \zeta) d\zeta, \quad i = 1, 2, 6$$

$$Q_i = \sum_{k=1}^N K_i^2 \int_{\zeta_{k-1}}^{\zeta_k} \alpha_i d\zeta, \quad i = 4, 5 \quad (9)$$

where N is the number of layers in the shell, ζ_k and ζ_{k-1} are the top and bottom ζ -coordinates of the k -th lamina, and K_i are the shear correction factors.

The strain-displacement equations of a shell are an approximation, within the assumptions made above, of the strain-displacement relations referred to orthogonal curvilinear coordinates. In addition, we assume that the transverse displacement u_3 does not vary with ζ . In the shear deformable theory of flat plates, we begin with the displacement field

$$\bar{u}_1 = \frac{1}{\alpha_1} (L_1 u_1) + \zeta \phi_1, \quad \bar{u}_2 = \frac{1}{\alpha_2} (L_2 u_2) + \zeta \phi_2, \quad \bar{u}_3 = u_3 \quad (10)$$

where $(\bar{u}_1, \bar{u}_2, \bar{u}_3)$ are the displacements of a point (ξ_1, ξ_2, ζ) along the (ξ_1, ξ_2, ζ) coordinates and (u_1, u_2, u_3) are the displacements of a point $(\xi_1, \xi_2, 0)$. A higher-order (in ζ) displacement field can be assumed in place of Eq. (10). Such theories have been considered by Whitney and Sun [23]. In the interest of brevity, although the procedures to be described can be applied to any higher-order theory, we consider only this first-order shear deformation theory. Substituting Eq. (10) into the strain-displacement relations of a orthogonal curvilinear coordinate system, and assuming that α_i are constant (to specialize the results to doubly-curve shells) one obtains

$$\epsilon_1 = \epsilon_1^0 + \zeta \kappa_1$$

$$\epsilon_2 = \epsilon_2^0 + \zeta \kappa_2$$

$$\begin{aligned}
 \epsilon_4 &= \epsilon_4^0 \\
 \epsilon_5 &= \epsilon_5^0 \\
 \epsilon_6 &= \epsilon_6^0 + \zeta \kappa_6
 \end{aligned} \tag{11}$$

where

$$\begin{aligned}
 \epsilon_1^0 &= \frac{1}{\alpha_1} \frac{\partial u_1}{\partial \xi_1} + \frac{u_3}{R_1} \\
 \epsilon_2^0 &= \frac{1}{\alpha_2} \frac{\partial u_2}{\partial \xi_2} + \frac{u_3}{R_2} \\
 \epsilon_4^0 &= \frac{1}{\alpha_2} \frac{\partial u_3}{\partial \xi_2} + \phi_2 - \frac{u_2}{R_2} \\
 \epsilon_5^0 &= \frac{1}{\alpha_1} \frac{\partial u_3}{\partial \xi_1} + \phi_1 - \frac{u_1}{R_1} \\
 \epsilon_6^0 &= \frac{1}{\alpha_1} \frac{\partial u_2}{\partial \xi_1} + \frac{1}{\alpha_2} \frac{\partial u_1}{\partial \xi_2} \\
 \kappa_1 &= \frac{1}{\alpha_1} \frac{\partial \phi_1}{\partial \xi_1} \\
 \kappa_2 &= \frac{1}{\alpha_2} \frac{\partial \phi_2}{\partial \xi_2} \\
 \kappa_6 &= \frac{1}{\alpha_1} \frac{\partial \phi_2}{\partial \xi_1} + \frac{1}{\alpha_2} \frac{\partial \phi_1}{\partial \xi_2} + \frac{1}{2} \left(\frac{1}{R_2} - \frac{1}{R_1} \right) \left(\frac{1}{\alpha_1} \frac{\partial u_2}{\partial \xi_1} - \frac{1}{\alpha_2} \frac{\partial u_1}{\partial \xi_2} \right)
 \end{aligned} \tag{12}$$

where ϕ_1 and ϕ_2 are the rotations of the reference surface $\zeta=0$ about the ξ_2 - and ξ_1 - coordinate axes, respectively. It should be noted that the displacement field in Eq. (10) can be used to derive the general shear deformation theory of laminated shells (i.e., α_i are not necessarily constant).

The stress-strain relations for the k-th orthotropic lamina in the material coordinate axes are given by

$$\begin{Bmatrix} \bar{\sigma}_1 \\ \bar{\sigma}_2 \\ \bar{\sigma}_4 \\ \bar{\sigma}_5 \\ \bar{\sigma}_6 \end{Bmatrix}^{(k)} = \begin{bmatrix} \bar{c}_{11} & \bar{c}_{12} & 0 & 0 & 0 \\ \bar{c}_{12} & \bar{c}_{22} & 0 & 0 & 0 \\ 0 & 0 & \bar{c}_{44} & 0 & 0 \\ 0 & 0 & 0 & \bar{c}_{55} & 0 \\ 0 & 0 & 0 & 0 & \bar{c}_{66} \end{bmatrix} \begin{Bmatrix} \bar{\epsilon}_1 \\ \bar{\epsilon}_2 \\ \bar{\epsilon}_4 \\ \bar{\epsilon}_5 \\ \bar{\epsilon}_6 \end{Bmatrix}^{(k)} \quad (13)$$

where \bar{c}_{ij} are the (plane stress-reduced) material stiffnesses of the lamina:

$$\bar{c}_{11} = \frac{E_1}{1-\nu_{12}\nu_{21}}, \quad \bar{c}_{12} = \frac{E_2\nu_{12}}{1-\nu_{12}\nu_{21}}, \quad \bar{c}_{22} = \frac{E_2}{1-\nu_{12}\nu_{21}}$$

$$\bar{c}_{44} = G_{23}, \quad \bar{c}_{55} = G_{13}, \quad \bar{c}_{66} = G_{12} \quad (14)$$

and

E_1, E_2 = Young's moduli in 1 and 2 material-principal directions, respectively

ν_{ij} = Poisson's ratio for transverse strain in the j -th direction when stressed in the i -th direction

G_{23}, G_{13}, G_{12} = shear moduli in the 2-3, 1-3, and 1-2 surfaces, respectively.

Poisson's ratios and Young's moduli are related by the reciprocal relations

$$\nu_{ij}E_j = \nu_{ji}E_i \quad (i = 1, 2). \quad (15)$$

The stress-strain relations (13) transformed to the shell coordinates become

$$\{\sigma\} = [Q^{(k)}]\{\epsilon\} \quad (16)$$

where $Q_{ij}^{(k)}$ are the material properties of k -th layer.

The principle of virtual work in the present case yields

$$\begin{aligned}
 0 &= \int_{-h/2}^{h/2} \int_{\Omega} [\sigma_1^{(k)} \delta \epsilon_1 + \sigma_2^{(k)} \delta \epsilon_2 + \sigma_6^{(k)} \delta \epsilon_6 + \sigma_4^{(k)} \delta \epsilon_4 + \sigma_5^{(k)} \delta \epsilon_5] \alpha_1 \alpha_2 d\xi_1 d\xi_2 d\zeta \\
 &= \int_{\Omega} [N_1 \delta \epsilon_1^0 + N_2 \delta \epsilon_2^0 + N_6 \epsilon_6^0 + M_1 \delta \kappa_1 + M_2 \delta \kappa_2 + M_6 \delta \kappa_6 + Q_1 \delta \epsilon_1^0 \\
 &\quad + Q_2 \delta \epsilon_2^0 - q \delta u_3] \alpha_1 \alpha_2 d\xi_1 d\xi_2 \quad (17)
 \end{aligned}$$

where q is the distributed transverse load.

The governing equations of equilibrium can be derived from Eq. (17) by integrating the displacement gradients in ϵ_i^0 by parts and setting the coefficients of δu_i ($i = 1, 2, 3$) and $\delta \phi_i$ ($i = 1, 2$) to zero separately. Thus one obtains

$$\begin{aligned}
 \frac{\partial N_1}{\partial x_1} + \frac{\partial}{\partial x_2} (N_6 + c_0 M_6) + \frac{Q_1}{R_1} &= 0 \\
 \frac{\partial}{\partial x_1} (N_6 - c_0 M_6) + \frac{\partial N_2}{\partial x_2} + \frac{Q_2}{R_2} &= 0 \\
 \frac{\partial Q_1}{\partial x_1} + \frac{\partial Q_2}{\partial x_2} - \left(\frac{N_1}{R_1} + \frac{N_2}{R_2} - q \right) &= 0 \\
 \frac{\partial M_1}{\partial x_1} + \frac{\partial M_6}{\partial x_2} - Q_1 &= 0 \\
 \frac{\partial M_6}{\partial x_1} + \frac{\partial M_2}{\partial x_2} - Q_2 &= 0 \quad (18)
 \end{aligned}$$

where c_0 denotes the constant

$$c_0 = \frac{1}{2} \left(\frac{1}{R_1} - \frac{1}{R_2} \right), \quad dx_j = \alpha_j d\xi_j. \quad (19)$$

This term is introduced by Sanders (see [18]), and distinguishes the Sanders theory from others. Using Eq. (13) in Eq. (8), the stress resultants (N_i, M_i, Q_i) can be related to (ϵ_i^0, κ_i) by

$$\begin{aligned} N_i &= A_{ij} \epsilon_j^0 + B_{ij} \kappa_j \\ M_i &= B_{ij} \epsilon_j^0 + D_{ij} \kappa_j \end{aligned} \quad (i, j = 1, 2, 6)$$

$$\begin{aligned} Q_2 &= A_{44} \epsilon_4^0 + A_{45} \epsilon_5^0 \\ Q_1 &= A_{45} \epsilon_4^0 + A_{55} \epsilon_5^0 \end{aligned} \quad (20)$$

Here A_{ij} , B_{ij} , and D_{ij} ($i, j = 1, 2, 6$) denote the extensional, flexural-extensional coupling, and flexural stiffnesses:

$$(A_{ij}, B_{ij}, D_{ij}) = \sum_{k=1}^N \int_{\zeta_{k-1}}^{\zeta_k} Q_{ij}^{(k)}(1, \zeta, \zeta^2) d\zeta. \quad (21)$$

The equations of Love's first-approximation shell theory can be obtained by setting $c_0 = 0$ in Eq. (18). Equations (18) can be specialized to flat plates, cylindrical shells, and spherical shells, respectively, by setting $\frac{1}{R_1} = \frac{1}{R_2} = 0$, $\frac{1}{R_1} = 0$ and $R_2 = R$ (the x_1 -axis is taken along a generator of the cylinder), and $R_1 = R_2 = R$. The classical thin shell theory can be obtained by setting $\phi_1 = -\frac{\partial u_3}{\partial x_1} + \frac{u_1}{R_1}$, and $\phi_2 = \frac{\partial u_3}{\partial x_2} + \frac{u_2}{R_2}$.

CLOSED-FORM SOLUTIONS

The exact form of the spatial variation of the solution of Eqs. (18) can be obtained under the following conditions:

- (i) Symmetric or antisymmetric cross-ply laminates: i.e., laminates with

$$A_{16} = A_{26} = B_{16} = B_{26} = D_{16} = D_{26} = A_{45} = 0. \quad (22)$$

- (ii) Freely supported boundary conditions:

$$\begin{aligned} N_1(0, x_2) = N_1(a, x_2) = M_1(0, x_2) = M_1(a, x_2) &= 0 \\ u_3(0, x_2) = u_3(a, x_2) = u_2(0, x_2) = u_2(a, x_2) &= 0 \\ N_2(x_1, 0) = N_2(x_1, b) = M_2(x_1, 0) = M_2(x_1, b) &= 0 \\ u_3(x_1, 0) = u_3(x_1, b) = u_1(x_1, 0) = u_1(x_1, b) &= 0 \\ \phi_2(0, x_2) = \phi_2(a, x_2) = \phi_1(x_1, 0) = \phi_1(x_1, b) &= 0 \end{aligned} \quad (23)$$

- (iii) Sinusoidal (spatial) distribution of the transverse load:

$$q = \sum_{m,n} q_{mn} \sin \alpha x_1 \sin \beta x_2, \quad \alpha = \frac{m\pi}{a}, \quad \beta = \frac{n\pi}{b} \quad (24)$$

where a and b are the dimensions of the shell middle surface along the x_1 and x_2 axes, respectively.

The exact form of the spatial variation of u_i ($i = 1, 2, 3$) and ϕ_i ($i = 1, 2$) is given by

$$\begin{aligned} u_1(x_1, x_2) &= \sum_{m,n} U_{mn} \cos \alpha x_1 \sin \beta x_2 \\ u_2(x_1, x_2) &= \sum_{m,n} V_{mn} \sin \alpha x_1 \cos \beta x_2 \\ u_3(x_1, x_2) &= \sum_{m,n} W_{mn} \sin \alpha x_1 \sin \beta x_2 \\ \phi_1(x_1, x_2) &= \sum_{m,n} X_{mn} \cos \alpha x_1 \sin \beta x_2 \\ \phi_2(x_1, x_2) &= \sum_{m,n} Y_{mn} \sin \alpha x_1 \cos \beta x_2. \end{aligned} \quad (25)$$

Clearly, the solution satisfies the boundary conditions in Eq. (23).

Substitution of Eqs. (24) and (25) into Eq. (18) yields a set of five linear algebraic equations in terms of the unknown amplitudes U, V, W, X, and Y. These equations can be expressed in matrix form as

$$- [C]\{\Delta\} = \{F\} \quad (26)$$

for bending, and

$$- [C]\{\Delta\} = \omega^2[S]\{\Delta\} \quad (27)$$

for natural vibration. Here ω denotes the frequency of natural vibration, $\{\Delta\}$ and $\{F\}$ denote the columns

$$\{\Delta\}^T = \{U, V, W, X, Y\}, \quad \{F\}^T = \{0, 0, q_{mn}, 0, 0\}, \quad (28)$$

and $c_{ij} \equiv c_{ji}$ and $S_{ij} = S_{ji}$ are given by

$$c_{11} = -\alpha^2 A_{11} - \beta^2 A_{66} - c_0^2 \beta^2 D_{66} - \frac{A_{55}}{R_1^2} - 2c_0 \beta^2 B_{66}$$

$$c_{12} = -\alpha\beta(A_{12} + A_{66} - c_0^2 D_{66})$$

$$c_{13} = \alpha\left(\frac{A_{11}}{R_1} + \frac{A_{12}}{R_2} + \frac{A_{55}}{R_1}\right)$$

$$c_{14} = -\alpha^2 B_{11} - \beta^2 B_{66} - c_0 \beta^2 D_{66} + \frac{A_{55}}{R_1}$$

$$c_{15} = -\alpha\beta(B_{12} + B_{66} + c_0 D_{66})$$

$$c_{22} = -\alpha^2 A_{66} - \alpha^2 c_0^2 D_{66} - \beta^2 A_{22} - \frac{A_{44}}{R_2^2} + 2c_0 \alpha^2 B_{66}$$

$$\begin{aligned}
c_{23} &= \beta \left(\frac{A_{12}}{R_1} + \frac{A_{22}}{R_2} + \frac{A_{44}}{R_2} \right) \\
c_{24} &= -\alpha \beta (B_{66} - c_0 D_{66} + B_{12}) \\
c_{25} &= -\alpha^2 (B_{66} - c_0 D_{66}) - \beta^2 B_{22} + \frac{A_{44}}{R_2} \\
c_{33} &= -A_{55} \alpha^2 - A_{44} \beta^2 - \frac{1}{R_1} \left(\frac{A_{11}}{R_1} + \frac{A_{12}}{R_2} \right) - \frac{1}{R_2} \left(\frac{A_{12}}{R_1} + \frac{A_{22}}{R_2} \right) \\
c_{34} &= \alpha \left(\frac{B_{11}}{R_1} + \frac{B_{12}}{R_2} - A_{55} \right) \\
c_{35} &= \beta \left(\frac{B_{12}}{R_1} + \frac{B_{22}}{R_2} - A_{44} \right) \\
c_{44} &= -\alpha^2 D_{11} - \beta^2 D_{66} - A_{55} \\
c_{45} &= -\alpha \beta (D_{12} + D_{66}) \\
c_{55} &= -\alpha^2 D_{66} - \beta^2 D_{22} - A_{44} \tag{29}
\end{aligned}$$

$$S_{11} = P_1 + 2P_2/R_1, \quad S_{14} = P_2, \quad S_{22} = P_1 + 2P_2/R_2, \quad S_{25} = P_2$$

$$S_{23} = P_1, \quad S_{44} = S_{55} = P_1, \quad \text{all other } S_{ij} = 0. \tag{30}$$

where

$$(P_1, P_2, P_3) = \sum_{k=1}^N \int_{\zeta_{k-1}}^{\zeta_k} \rho^{(k)}(1, \zeta, \zeta^2) d\zeta \tag{31}$$

$\rho^{(k)}$ being the density of the k -th layer.

Similar calculation for antisymmetric angle-ply shells ($A_{16} = A_{26} = B_{11} = B_{12} = B_{22} = B_{66} = D_{16} = D_{26} = A_{45} = 0$) with the solution of the form

$$\begin{aligned}
u_1(x_1, x_2) &= \sum_{m,n} U_{mn} \sin \alpha x_1 \cos \beta x_2 \\
u_2(x_1, x_2) &= \sum_{m,n} V_{mn} \cos \alpha x_1 \sin \beta x_2
\end{aligned} \tag{32}$$

and u_3 , ϕ_1 , and ϕ_2 as given in Eq. (25), shows that the exact solution is possible if and only if $1/R_1 = 1/R_2 = 0$. In other words, antisymmetric angle-ply plates admit exact solutions but shells do not. To see this, substitute Eq. (24), last three of Eq. (25), and Eq. (32) into Eq. (18). Note that the assumed solution satisfies the following type of simply supported boundary conditions.

$$\begin{aligned}
N_6(0, x_2) &= N_6(a, x_2) = N_6(x_1, 0) = N_6(x_1, b) = 0 \\
u_1(0, x_2) &= u_1(a, x_2) = u_2(x_1, 0) = u_2(x_1, b) = 0 \\
u_3(0, x_1) &= u_3(a, x_2) = u_3(x_1, 0) = u_3(x_1, b) = 0 \\
\phi_1(x_1, 0) &= \phi_1(x_1, b) = \phi_2(0, x_2) = \phi_2(a, x_2) = 0 \\
M_2(x_1, 0) &= M_2(x_1, b) = M_1(0, x_2) = M_1(a, x_2) = 0
\end{aligned} \tag{33}$$

From the first equation in Eq. (18), we obtain

$$\begin{aligned}
&\{[-2\alpha\beta(A_{16} + c_0 B_{16})]U_{mn} + [-\alpha^2(A_{16} - c_0 B_{16}) - \beta^2(A_{26} + c_0 B_{26}) - \frac{A_{45}}{R_1 R_2}]V_{mn} \\
&+ [\frac{A_{11}}{R_1} + \frac{A_{12}}{R_2} + \frac{A_{55}}{R_1}] \alpha W_{mn} + [-\alpha^2 B_{11} - \beta^2(B_{66} + c_0 D_{66}) + \frac{A_{55}}{R_1}] X_{mn} \\
&+ [-\alpha\beta(B_{12} + B_{66} + c_0 D_{66})] Y_{mn}\} \cos \alpha x_1 \sin \beta x_2 \\
&+ \{[-\alpha^2 A_{11} - \beta^2(A_{66} + 2c_0 B_{66} + c_0^2 D_{66}) - \frac{A_{55}}{R_1^2}]U_{mn} + [-\alpha\beta(A_{12} + A_{66} + 2c_0 B_{66} + c_0^2 D_{66})]V_{mn} \\
&+ [\frac{A_{16} + c_0 B_{16}}{R_1} + \frac{A_{26} + c_0 B_{26}}{R_2} + \frac{A_{45}}{R_1}] \beta W_{mn} + [-\alpha\beta(2B_{16} + c_0 D_{16})] X_{mn} \\
&+ [-\alpha^2 B_{16} - \beta^2(B_{26} + c_0 D_{26}) + \frac{A_{45}}{R_1}] Y_{mn}\} \sin \alpha x_1 \cos \beta x_2 = 0
\end{aligned} \tag{34}$$

For antisymmetric angle-ply laminates, the following stiffnesses are identically zero:

$$A_{16} = A_{26} = B_{11} = B_{12} = B_{22} = B_{66} = D_{16} = D_{26} = A_{45} = 0 \quad (35)$$

As a result Eq. (34) reduces to

$$\begin{aligned} & [-2\alpha\beta c_0 B_{16} U_{mn} + c_0(\alpha^2 B_{16} - \beta^2 B_{26}) V_{mn} + \alpha(\frac{A_{11}}{R_1} + \frac{A_{12}}{R_2} + \frac{A_{55}}{R_1}) W_{mn} \\ & + (-\beta^2 c_0 D_{66} \epsilon \frac{A_{55}}{R_1} X_{mn} - \alpha\beta c_0 D_{66} Y_{mn}) \cos\alpha x_1 \sin\beta x_2 \\ & + \{[-\alpha^2 A_{11} - \beta^2(A_{66} + c_0^2 D_{66}) - \frac{A_{55}}{R_1^2}] U_{mn} + [-\alpha\beta(A_{12} + A_{66} + c_0^2 D_{66})] V_{mn} \\ & + \beta c_0(\frac{B_{16}}{R_1} + \frac{B_{26}}{R_2}) W_{mn} - 2\alpha\beta R_{16} X_{mn} - (\alpha^2 R_{16} + \beta^2 R_{26}) Y_{mn} \} \sin\alpha x_1 \cos\beta x_2 = 0 \end{aligned} \quad (36)$$

Thus, we get two equations, by setting the coefficients of $\cos\alpha x_1 \sin\beta x_2$ and $\sin\alpha x_1 \cos\beta x_2$ to zero, from the first equilibrium equation. Similarly, we obtain eight more equations from the remaining four equilibrium equations. In other words, we have ten equations in five unknowns ($U_{mn}, V_{mn}, W_{mn}, X_{mn}, Y_{mn}$), which have no unique solution. These ten equations reduce to five when $1/R_1$ and $1/R_2$ are set to zero, as can be seen from Eq. (36). Thus antisymmetric angle-ply shells do not admit exact solution while antisymmetric angle-ply plates do.

NUMERICAL RESULTS

As a first example of bending, a doubly curved shell under transverse concentrated load at the center is analyzed. The following geometric^{and} material parameters are used:

$$\begin{aligned} R_1 = R_2 = 96.0 \text{ in.}, \quad a = b = 32.0 \text{ in.}, \quad h = 0.1 \text{ in.}, \\ E_1 = E_2 = 10^7 \text{ psi}, \quad \nu = 0.3, \quad \text{intensity of load} = 100 \text{ lb.} \end{aligned} \quad (37)$$

This problem was also solved using the finite element method by Yang [27]. Table 1 contains the center transverse deflection obtained using the shear deformation theory (SDT) and classical shell theory (CST) for various terms in the series. The numerical solution of Vlasov [20] is taken from Yang's paper. It should be pointed out that both Vlasov and Yang did not consider transverse shear strains. It is clear from the results that the series solution converges very slowly. The difference between the values predicted by SDT and CST theories is not significant because the ratios $a/h = 320$ and $R/h = 960$ are very large (hence, the shell is essentially very thin and shallow).

To investigate the effect of transverse shear strains on the center deflection, the same spherical shell problem with point load at the center or uniformly distributed loading are analyzed, and the results are presented in Table 2. Note that for uniformly distributed load, the solution given by the 50-term series is the same as that given by the 250-term series, indicating that the convergence is achieved with 50 (or less) terms in the series. Comparison of the SDT results with the CST results show that the shear deformation is significant for side to thickness ratios smaller than 10. For example, the classical theory solution differs from the shear deformation theory solution by 0.35% for $a/h = 20$, 3.6% for $a/h = 10$, and 18.6% for $a/h = 5$.

TABLE 1. Center transverse deflection of a spherical shell under point load at the center ($R_1 = R_2 = 96$ in: $a = b = 32$ in., $h = 0.1$, $E = 10^7$ psi, $\nu = 0.3$, load, $P = 100$ lbs)

Theory	n*=9	n=49	n=99	n=149	n=199	n=249
SDT	0.032594	0.039469	0.03972	0.039786	0.039814	0.039832
CST	-	-	0.03959	-	0.039647	0.039653
Vlasov [20]	-	-	0.03956	-	-	-

* nxn-term series; finite-element solution of Yang [27]: 0.03867

TABLE 2. Center transverse deflection ($w \times 10^3$) of spherical shells under point load at the center and uniformly distributed load (see Table 1 for the problem data).

h	n=9	n=49	n=99	n=149	n=199	n=249
Point load at the center						
0.32	3.664	3.9019	3.9194	3.9270	3.9319	3.9356
1.60	0.1646	0.1713	0.1735	0.1748	0.1757	0.1764
3.20	0.0349	0.0376	0.0386	0.0393	0.0397	0.0400
6.40	0.0067	0.0080	0.0085	0.0088	0.0091	0.0092
Uniformly distributed load						
0.32	314.28 (314.33)*	313.87 (313.93)	313.86 (313.93)	313.86 (313.93)	313.86	313.86
1.60	49.701 (49.526)	49.695 (49.523)	49.695 (49.523)	49.695 (49.523)	49.695	49.695
3.20	11.266 (10.873)	11.265 (10.872)	11.265 (10.872)	11.265 (10.872)	11.265	11.265
6.40	1.9774 (1.6669)	1.9767 (1.6669)	1.9767 (1.6669)	1.9767 (1.6669)	1.9767	1.9767

* CST solution

TABLE 3. Nondimensionalized center deflection* versus radius to thickness ratio for cross-ply spherical shells under sinusoidally distributed transverse loads. ($a/b = 1.0$; material: $E_1/E_2 = 25$, $G_{23} = 0.2E_2$, $G_{13} = G_{12} = 0.5E_2$)

R/a	0°/90°		0°/90°/0°		0°/90°/90°/0°	
	a/h=100	a/h=10	a/h=100	a/h=10	a/h=100	a/h=10
1	0.0536	4.023	0.0536	3.2590	0.0532	3.2290
2	0.2111	8.156	0.2068	5.3052	0.2054	5.2542
3	0.4634	10.062	0.4391	5.9971	0.4362	5.9387
4	0.7969	10.958	0.7237	6.2834	0.7192	6.2219
5	1.1948	11.429	1.0337	6.4253	1.0279	6.3623
10	3.5760	12.123	2.4109	6.6247	2.4030	6.5595
10 ³⁰	10.653	12.373	4.3370	6.6939	4.3368	6.6280

* $\bar{w} = (wn^3E_2/q_0a^4) \times 10^3$; q_0 = intensity of the transverse load

TABLE 4. Nondimensional center deflection versus radius to thickness ratio of spherical shells under uniformly distributed load (19-term solution)

R/a	0°/90°		0°/90°/0°		0°/90°/90°/0°	
	a/h=100	a/h=10	a/h=100	a/h=10	a/h=100	a/h=10
1	0.0718	6.054	0.0718	4.8173	0.0715	4.8366
2	0.2855	12.668	0.2858	8.0210	0.2844	8.0517
3	0.6441	15.739	0.6224	9.1148	0.6246	9.1463
4	1.1412	17.184	1.0443	9.5686	1.0559	9.5999
5	1.7535	19.944	1.5118	9.7937	1.5358	9.8249
10	5.5428	19.065	3.6445	10.110	3.7208	10.141
10 ³⁰	16.980	19.469	6.6970	10.220	6.8331	10.251

Next, the results of bending of cross-ply laminated shells are discussed. The same geometric parameters as used in the isotropic shells are also used for composite shells. Individual layers are assumed to be orthotropic, with the following properties:

$$E_1 = 25E_2, G_{23} = 0.2E_2, G_{13} = G_{12} = 0.5E_2, \nu_{12} = 0.25 \quad (38)$$

Tables 3-5 contain nondimensionalized center transverse deflections of cross-ply spherical shells under sinusoidal, uniformly distributed, and point loads, respectively. The results are tabulated for various ratios of radius to thickness and for two values of side to thickness. From these results it follows that the center deflection varies rapidly with the ratio R/h for deep shells (i.e., for large ratios of a/h) than for shallow shells (i.e., for small ratios of a/h).

The present solution can also be applied to special laminates, $[0^\circ/\pm 45^\circ]_{\text{sym}} \equiv [0^\circ/45^\circ/-45^\circ/-45^\circ/45^\circ/0^\circ]$, which are used in F-16 aircraft by General Dynamics Corporation, Ft. Worth. For the scheme, $[0^\circ/\pm 45^\circ]_{\text{sym}}$, we have $A_{16} = A_{26} = D_{16} = D_{26} = B_{ij} = 0$ and therefore the solution developed in the present study applies. Table 6 contains the nondimensionalized center deflections for cylindrical and spherical shells with various side to thickness ratios and radius to side ratios.

To complete the analysis, the results of free vibration are also presented. Tables 7 and 8 contain nondimensionalized fundamental frequencies for spherical ($R_1 = R_2$) and cylindrical shells ($R_1 = 10^3 R_2$), respectively.

Two sets of shear correction factors were used to investigate their influence on the fundamental frequencies. For a fixed ratio of R/a , the shear correction factors have little or no effect on the frequencies for $a/h = 100$.

For $a/h = 10$, the effect of smaller values of shear correction factors is to lower the frequencies, the rate of decrease being the highest for the four-layer cross-ply. For identical lamination and geometry, spherical shells have higher natural frequencies than cylindrical shells.

TABLE 5. Nondimensionalized center deflection* versus radius to side ratio of spherical shells under point load at the center (101-term solution)

R/a	0°/90°	0°/90°/0°	0°/90°/90°/0°
10	4.0164	3.7127	3.5815
20	5.7620	4.6502	4.4678
30	6.5444	4.9546	4.7579
40	6.9098	5.0794	4.8771
50	7.1015	5.1410	4.9360
100	7.3836	5.2273	5.0186
10 ³⁰	7.4853	5.2572	5.0472

$$* \bar{w} = \left(\frac{wh^3 E_2}{Pa^2} \right) \times 10^2 ; \quad a/b = 1, \quad a/h = 10, \quad P = \text{point load}$$

TABLE 6. Nondimensional center deflections of simply supported, special laminates $[0^\circ/\pm 45^\circ]_{\text{sym}}$ cylindrical and spherical shells.

a/h R/a	Sinusoidal loading			Uniform loading*		
	5	10	100	5	10	100
Cylindrical Shell (R/a = 2)						
2	9.4976	4.1168	0.1623	14.0224	6.1794	0.0928
4	10.5152	4.9927	0.5697	15.6616	7.5956	0.733
Spherical Shell ($R_1 = R_2 = R$, R/a = 2)						
2	6.7850	2.4120	0.0421	9.7344	3.4794	0.0391
4	9.468	4.1117	0.1623	13.9936	6.1856	0.1930

* 51-term solution

TABLE 7 Nondimensionalized fundamental frequencies, $\bar{\omega} = \omega a^2 \sqrt{\rho/E_2}/h$, versus radius to side length ratio of spherical shell ($a/b=1$).

R/a	0°/90°		0°/90°/0°		0°/90°/90°/0°	
	a/h=100	a/h=10	a/h=100	a/h=10	a/h=100	a/h=10
1	125.93	14.481	125.99	16.115	126.33	16.172
	125.93	14.420	125.99	15.746	126.33	15.827
2	67.362	10.749	68.075	13.382	68.294	13.447
	67.361	9.5161	68.072	12.794	68.291	12.867
3	46.002	9.9608	47.265	12.731	47.415	12.795
	46.001	9.6473	47.260	12.077	47.410	12.178
4	35.228	9.4102	36.971	12.487	37.082	12.552
	35.227	9.2644	36.964	11.808	37.075	11.910
5	28.825	9.2309	30.993	12.372	31.079	12.437
	28.825	9.0791	30.986	11.680	31.071	11.783
10	16.706	8.9841	20.347	12.215	20.380	12.280
	16.704	8.8225	20.335	11.506	20.368	11.609
10 ³⁰	9.6873	8.8998	15.183	12.162	15.184	12.226
	9.6850	8.7317	15.167	11.447	15.168	11.551

[†] the first line of values corresponds to $K_1^2 = K_2^2 = 5/5$, and the second line corresponds to $K_1^2 = 0.7$, $K_2^2 = 0.6$.

Table 8 Nondimensionalized fundamental frequencies versus radius to side length of cylindrical shells ($a/b = 1$, $R_1 = 10^{30}$).

R ₂ /a	0°/90°		0°/90°/0°		0°/90°/90°/0°	
	a/h=100	a/h=10	a/h=100	a/h=10	a/h=100	a/h=10
1	65.474	9.9986	66.583	13.172	66.704	13.128
	65.473	9.9018	66.580	12.578	66.700	12.567
2	34.914	9.1476	36.770	12.438	36.858	12.471
	34.913	9.0098	36.763	11.758	36.851	11.828
3	24.516	8.9832	27.116	12.287	27.173	12.337
	24.515	8.8832	27.106	11.587	27.164	11.676
4	19.509	8.9301	22.709	12.233	22.749	12.289
	19.508	8.7746	22.698	11.526	22.738	11.622
5	16.668	8.9082	20.332	12.207	20.361	12.267
	16.667	8.7498	20.320	11.498	20.349	11.596
10	11.831	8.8879	16.625	12.173	16.634	12.236
	11.829	8.7241	16.610	11.459	16.619	11.562
10 ³⁰ (plate)	9.6873	8.8998	15.183	12.162	15.184	12.226
	9.6850	8.7317	15.167	11.447	15.168	11.551

CONCLUSIONS

Closed-form solutions for deflections and natural frequencies of simply supported, cross-ply laminated and quasi-isotropic shells are derived using the shear deformation version, developed herein, of the Sanders shell theory. Unlike plates, antisymmetric angle-ply shells do not admit exact solutions. The exact solutions presented herein for cylindrical and spherical cross-ply shells under sinusoidal, uniformly distributed, and point loads should serve as bench mark results for approximate methods, such as the finite element and finite difference methods.

Acknowledgment

The results presented in this paper were obtained during an investigation supported by the Air Force Office of Scientific Research, Bolling Air Force Base (Grant AFOSR-81-0142). The author is thankful to Professor C. W. Bert for his comments on an earlier version of this manuscript.

REFERENCES

1. S. A. Ambartsumyan, Theory of Anisotropic Shells, Moscow, 1961; English translation, NASA TT F 118, May 1964.
2. S. A. Ambartsumyan, "Calculation of Laminated Anisotropic Shells," Izvestiia Akademiia Nauk Armenskoi SSR, Ser. Fiz. Mat. Est. Tekh. Nauk., Vol. 6, No. 3, 1953, p. 15.
3. C. W. Bert and P. H. Francis, "Composite Material Mechanics: Structural Mechanics," AIAA Journal, Vol. 12, No. 9, 1974, pp. 1173-1186.
4. C. W. Bert, "Analysis of Shells," Structural Design and Analysis, Part I, C. C. Chamis (ed.), Vol. 7 of Composite Materials, L. J. Broutman and R. H. Krock (eds.), Wiley, New York, 1974, pp. 207-258.
5. C. W. Bert and T. L. C. Chen, "Effect of Shear Deformation on Vibration of Antisymmetric Angle-Ply Laminated Rectangular Plates," Int. J. Solids and Structures, Vol. 14, 1978, pp. 465-473.
6. C. W. Bert, and M. Kumar, "Vibration of Cylindrical Shells of Bimodulus Composite Materials," J. Sound and Vibration, Vol. 81, No. 1, 1982, pp. 107-121.
7. C. W. Bert and V. S. Reddy, "Cylindrical Shells of Bimodulus Material," Journal of Engineering Mechanics Division, Proc. ASCE, Vol. 8, No. EM5, 1982, pp. 675-688.
8. S. Cheng and R. P. Ho, "Stability of Heterogeneous Anisotropic Cylindrical Shells Under Combined Loading," AIAA Journal, Vol. 1, No. 4, 1963, pp. 892-898.
9. S. B. Dong, K. S. Pister, and R. L. Taylor, "On the Theory of Laminated Anisotropic Shells and Plates," Journal of Aerospace Sciences, Vol. 29, 1962, pp. 969-975.
10. L. H. Donnell, "Stability of Thin Walled Tubes in Torsion," NACA Report 479, 1933.
11. W. Flugge, Stresses in Shells, Springer, Berlin, 1960.
12. S. T. Gulati and F. Essenberg, "Effects of Anisotropy in Axisymmetric Cylindrical Shells," Journal of Applied Mechanics, Vol. 34, 1967, pp. 650-666.
13. Y. S. Hsu, J. N. Reddy and C. W. Bert, "Thermoelasticity of Circular Cylindrical Shells Laminated of Bimodulus Composite Materials," Journal of Thermal Stresses, Vol. 4, 1981, pp. 155-177.
14. H. Kraus, Thin Elastic Shells, John Wiley, N.Y., 1967.

15. A. E. H. Love, "On the Small Free Vibrations and Deformations of the Elastic Shells," Philosoph. Trans. Royal Soc., (London), Ser. A, Vol. 17, 1888, pp. 491-546.
16. P. M. Naghdi, "A Survey of Recent Progress in the Theory of Elastic Shells," Appl. Mech. Reviews, Vol. 9, No. 9, 1956, pp. 365-368.
17. J. N. Reddy and W. C. Chao, "A Comparison of Closed-Form and Finite Element Solutions of Thick, Laminated, Anisotropic Rectangular Plates," Nuclear Engng. and Design, Vol. 64, 1981, pp. 153-167.
18. J. L. Sanders, Jr., "An Improved First-Approximation Theory for Thin Shells," NASA Technical Report R-24, 1959.
19. Y. Stavsky, "Thermoelasticity of Heterogeneous Anisotropic Plates," J. Engng. Mech. Div., Proc. ASCE, Vol. 89, FM2, 1963, pp. 89-105.
20. V. Z. Vlasov, General Theory of Shells and Its Applications in Engineering, (Translation of *Obshchaya teoriya obolochek i yeye prilozheniya v tekhnike*), NASA TT F-99, Nat. Aeron. and Space Adm., Washington, D.C. 1964.
21. J. M. Whitney, and A. W. Leissa, "Analysis of Heterogeneous Anisotropic Plates," J. Appl. Mech., Vol. 36, 1969, pp. 261-266.
22. J. M. Whitney and N. J. Pagano, "Shear Deformation in Heterogeneous Anisotropic Plates," J. Appl. Mech., Vol. 37, 1970, pp. 1031-1036.
23. J. M. Whitney and C. T. Sun, "A higher order theory for extensional motion of laminated anisotropic shells and plates," J. Sound and Vibration, Vol. 30, 1973, p. 85.
24. J. M. Whitney, and C. T. Sun, "A Refined Theory for Laminated Anisotropic Cylindrical Shells," Journal of Applied Mechanics, Vol. 41, 1974, pp. 471-476.
25. G. E. O. Widera and S. W. Chung, "A Theory for Non-Homogeneous Anisotropic Cylindrical Shells," Journal of Applied Mathematics & Physics, (ZAMP), Vol. 21, pp. 1970, 378-399.
26. G. E. O. Widera and D. L. Logan, "Refined Theories for Nonhomogeneous Anisotropic Cylindrical Shells: Part I-Derivation," Journal of the Engineering Mechanics Division, Proc. ASCE, Vol. 106, No. EM6, 1980, pp. 1053-1074.
27. T. Y. Yang, "High Order Rectangular Shallow Shell Finite Element," J. Engineering Mechanics Division, Proc. ASCE, Vol. 99, EM1, 1973, pp. 57-181.
28. J. A. Zukas, and J. R. Vinson, "Laminated Transversely Isotropic Cylindrical Shells," Journal of Applied Mechanics, Vol. 38, 1971, pp. 400-407.

APPENDIX II. - NOTATION

The following symbols are used in this paper:

A_{ij}	= extensional stiffness; see Eq. (21)
a	= curvilinear dimension of the laminate along the ξ_1 -axis
dA_1, dA_2	= area elements perpendicular to the ξ_1 and ξ_2 axes
B_{ij}	= bending-extensional stiffness; see Eq. (21)
b	= curvilinear dimension of the laminate along the ξ_2 -axis
c_{ij}	= coefficients defined in Eq. (29)
\bar{c}_{ij}	= plane-stress-reduced material stiffness of the lamina
D_{ij}	= bending stiffnesses; see Eq. (21)
E_1, E_2	= Young's moduli in 1 and 2 material principal directions
G_{ij}	= shear moduli in the i - j surfaces, respectively
h	= thickness of the shell
L_i	= Lamé coefficients ($i = 1, 2, 3$)
M_i	= moment resultants ($i = 1, 2, 6$); see Eqn. (9)
m	= number of terms in the series (24) and (25)
N	= total number of layers in the laminate
N_i	= normal stress resultants ($i = 1, 2, 6$); see Eqn. (9)
n	= number of terms in the series (24) and (26)
P_i	= rotary, and coupled-rotary inertias defined in Eqn. (31)
Q_i	= shear stress resultants ($i = 1, 2$); see Eqn. (9)
q_{mn}	= coefficients in the expansion of the transverse load; see Eq. (24)
\underline{r}	= position vector of a point in the shell
R_i	= principal radii of curvature; see Fig. 1
\underline{r}	= position vector of a point on the shell midsurface

S_{ij}	= the mass coefficients defined in Eqn. (30)
U_{mn}	= amplitudes of displacement u_1 ; see Eqn. (25)
u_i	= displacements of the midsurface
\bar{u}_i	= displacements of a point in the shell
V_{mn}	= amplitudes of displacement u_2 ; see Eqn. (25)
W_{mn}	= amplitudes of displacement u_3
X_{mn}	= amplitudes of rotation ϕ_1
Y_{mn}	= amplitudes of rotation ϕ_2
α	= $m\pi/a$
α_i	= surface metrics ($i = 1,2$) defined in Eq. (2)
β	= $n\pi/b$
δ	= variational operator
ϕ_i	= rotations about normal to the shell midsurface
ϵ_i	= strain components ($i = 1,2,4,5,6$); see Eqn. (11)
σ_i	= stress components ($i = 1,2,4,5,6$)
ξ_i	= curvilinear coordinates in the surface of the shell
ζ	= coordinate transverse to the shell midsurface
ν_{ij}	= Poisson's ratios

KEY WORDS

Laminated Shells

Angle-Ply

Bending

Cross-Ply

Doubly-Curved Shells

Exact Solutions

Transverse Shear

Vibration

Shear Deformation Theory

WP:ASCER3

GEOMETRICALLY NONLINEAR ANALYSIS OF LAMINATED SHELLS
INCLUDING TRANSVERSE SHEAR STRAINS

J. N. Reddy and K. Chandrashekara

Department of Engineering Science and Mechanics
Virginia Polytechnic Institute and State University
Blacksburg, VA 24061

ABSTRACT

The paper contains a description of a doubly curved shell finite element for geometrically nonlinear (in the von Karman sense) analysis of laminated (doubly-curved) composite shells. The element is based on an extension of the Sanders shell theory and accounts for the von Karman strains and transverse shear strains. The numerical accuracy and convergence characteristics of the element are further evaluated by comparing the present results for the bending of isotropic and orthotropic plates and shells with those available in the literature. The many numerical results presented here for the geometrically nonlinear analysis of laminated composite shells should serve as reference for future investigations.

INTRODUCTION

Laminated shells are finding increased application in aerospace, automobile and petrochemical industries. This is primarily due to the high stiffness to weight ratio, high strength to weight ratio, and less machining and maintenance costs associated with composite structures. However, the analysis of composite structures is more complicated when compared to metallic structures, because laminated composite structures are anisotropic and characterized by bending-stretching coupling. Further, the classical shell theories, which are based on the Kirchoff-Love kinematic hypothesis (see Naghdi [1] and

Bert [2]) are known to yield deflections and stresses in laminated shells that are as much as 30% in error. This error is due to the neglect of transverse shear strains in the classical shell theories.

Refinements of the classical shell theories (e.g., Love's first approximation theory [3]) for shells to include transverse shear deformation have been presented by Reissner [4-6]. Sanders [7] presented modified first- and second-approximation theories that removed an inconsistency (nonvanishing of a small rigid-body rotations of the shell) existed in Love's first-approximation theory.

The first thin shell theory of laminated orthotropic composite shells is due to Ambartsumyan [8,9]. In these works Ambartsumyan assumed that the individual orthotropic layers were oriented such that the principal axes of material symmetry coincided with the principal coordinates of the shell reference surface. Dong, Pister, and Taylor [10] presented an extension of Donnell's shallow shell theory [11] to thin laminated shells. Using the asymptotic integration of the elasticity equations, Widera and Chung [12] derived a first-approximation theory for the unsymmetric deformation of nonhomogeneous, anisotropic, cylindrical shells. This theory, when specialized to isotropic materials, reduces to Donnell's shell theory.

The effects of transverse shear deformation and thermal expansion through the shell thickness were considered by Zukas and Vinson [13]. Dong and Tso [14] constructed a laminated orthotropic shell theory that includes transverse shear deformation. This theory can be regarded as an extension of Love's first-approximation theory [3] for homogeneous isotropic shells. Other refined theories, specialized to anisotropic cylindrical shells, were presented by Whitney and Sun [15], and Widera and Logan [16,17].

The finite-element analysis of layered anisotropic shells, all of which are concerned with bending, stability, or vibration of shells, can be found in the works of Schmit and Monforton [18], Panda and Natarajan [19], Shivakumar and Krishna Murty [20], Rao [21], Siede and Chang [22], Hsu, Reddy, and Bert [23], Reddy [24], and Venkatesh and Rao [25,26]. Recently, Reddy [27] extended the Sanders theory to account for the transverse shear strains, and presented exact solutions for simply supported cross-ply laminated shells. All of these studies are limited small displacement theories and static analyses.

In the present paper, an extension of the Sanders shell theory that accounts for the shear deformation and the von Karman strains in laminated anisotropic shells is used to develop a displacement finite element model for the bending analysis of laminated composite shells. The accuracy of the element is evaluated by comparing the results obtained in the present study for isotropic and orthotropic plate and shell problems with those available in the literature. Numerical results for bending analysis of cylindrical and doubly-curved shells are presented, showing the effect of radius-to-thickness ratio, loading, and boundary conditions on the deflections and stresses.

A REVIEW OF THE GOVERNING EQUATIONS

Consider a laminated shell constructed of a finite number of uniform-thickness orthotropic layers, oriented arbitrarily with respect to the shell coordinates (ξ_1, ξ_2, ζ) . The orthogonal curvilinear coordinate system (ξ_1, ξ_2, ζ) is chosen such that the ξ_1 - and ξ_2 - curves are lines of curvature on the midsurface $\zeta=0$, and ζ -curves are straight lines perpendicular to the surface $\zeta=0$ (see Fig. 1). A line element of the shell is given by (see Reddy [27])

$$(dS)^2 = [(1 + \zeta/R_1)\alpha_1 d\xi_1]^2 + [(1 + \zeta/R_2)\alpha_2 d\xi_2]^2 + (d\zeta)^2 \quad (1)$$

where α_i and R_i ($i = 1, 2$) are the surface metrics and radii of curvature, respectively. In general, α_i and R_i are functions of ξ_i only. For the doubly curved shells considered in the present theory, α_i and R_i are constant.

The strain-displacement equations of the shear deformable theory of doubly-curved shells are given by

$$\begin{aligned}\epsilon_1 &= \epsilon_1^0 + \zeta \kappa_1 \\ \epsilon_2 &= \epsilon_2^0 + \zeta \kappa_2 \\ \epsilon_4 &= \epsilon_4^0 \\ \epsilon_5 &= \epsilon_5^0 \\ \epsilon_6 &= \epsilon_6^0 + \zeta \kappa_6\end{aligned}\quad (2)$$

where

$$\begin{aligned}\epsilon_1^0 &= \frac{\partial u_1}{\partial x_1} + \frac{u_3}{R_1} + \frac{1}{2} \left(\frac{\partial u_3}{\partial x_1} \right)^2, \quad \kappa_1 = \frac{\partial \phi_1}{\partial x_1} \\ \epsilon_2^0 &= \frac{\partial u_2}{\partial x_2} + \frac{u_3}{R_2} + \frac{1}{2} \left(\frac{\partial u_3}{\partial x_2} \right)^2, \quad \kappa_2 = \frac{\partial \phi_2}{\partial x_2} \\ \epsilon_6^0 &= \frac{\partial u_1}{\partial x_2} + \frac{\partial u_2}{\partial x_1} + \frac{\partial u_3}{\partial x_1} \frac{\partial u_3}{\partial x_2}, \quad \kappa_6 = \frac{\partial \phi_1}{\partial x_2} + \frac{\partial \phi_2}{\partial x_1} + c_0 \left(\frac{\partial u_2}{\partial x_1} - \frac{\partial u_1}{\partial x_2} \right) \\ \epsilon_4^0 &= \phi_2 + \frac{\partial u_3}{\partial x_2} - \frac{u_2}{R_2} \\ \epsilon_5^0 &= \phi_1 + \frac{\partial u_3}{\partial x_1} - \frac{u_1}{R_1} \\ c_0 &= \frac{1}{2} \left(\frac{1}{R_2} - \frac{1}{R_1} \right)\end{aligned}\quad (3)$$

Here u_i denotes the displacements of the reference surface along ξ_i ($\xi_3 = \zeta$) axes, and ϕ_i are the rotations of the transverse normals to the reference surface. In Love's first-approximation theories the parameter c_0 is taken to be zero, and it is introduced only in the Sanders theory.

The stress-strain relations, transformed to the shell coordinates, are of the form

$$\{\sigma\} = [Q]\{\epsilon\} \quad (4)$$

where $Q_{ij}^{(k)}$ are the material properties of k-th layer.

The principle of virtual work for the present problem is given by

$$0 = \sum_{k=1}^L \int_{\zeta_{k-1}}^{\zeta_k} \int_{\Omega} \{ \sigma_1^{(k)} \delta \epsilon_1 + \sigma_2^{(k)} \delta \epsilon_2 + \sigma_6^{(k)} \delta \epsilon_6 + \sigma_4^{(k)} \delta \epsilon_4 + \sigma_5^{(k)} \delta \epsilon_5 - q \delta u_3 \} \alpha_1 \alpha_2 d\zeta_1 d\zeta_2 d\zeta \quad (5)$$

$$= \int_{\Omega} [N_1 \delta \epsilon_1^0 + N_2 \delta \epsilon_2^0 + N_6 \epsilon_6^0 + M_1 \delta \kappa_1 + M_2 \delta \kappa_2 + M_6 \delta \kappa_6 + Q_1 \delta \epsilon_5^0 + Q_2 \delta \epsilon_4^0 - q \delta u_3] \alpha_1 \alpha_2 d\zeta_1 d\zeta_2 \quad (6)$$

where q is the distributed transverse load, N_i and M_i are the stress and moment resultants, and Q_i is the shear force resultant:

$$(N_i, M_i) = \sum_{k=1}^L \int_{\zeta_{k-1}}^{\zeta_k} \sigma_i(1, \zeta) d\zeta, \quad i = 1, 2, 6$$

$$Q_i = \sum_{k=1}^L K_i^2 \int_{\zeta_{k-1}}^{\zeta_k} \sigma_i d\zeta, \quad i = 4, 5, \quad (7)$$

where K_i ($i = 1, 2$) are the shear correction factors (taken to be $K_1^2 = K_2^2 = 5/6$), and (ζ_{k-1}, ζ_k) are the ζ -coordinates of the k-th layer, and L is the total number of layers in the laminated shell.

It is informative to note that the equations of equilibrium can be derived from Eq. (6) by integrating the displacement gradients in ϵ_i^0 by parts

and setting the coefficients of δu_i ($i = 1, 2, 3$) and $\delta \phi_i$ ($i=1, 2$) to zero separately. We obtain [with $c_0 = \frac{1}{2} (\frac{1}{R_2} - \frac{1}{R_1})$ and $dx_i = \alpha_i d\xi_i$]

$$\begin{aligned} \frac{\partial N_1}{\partial x_1} + \frac{\partial}{\partial x_2} (N_6 - c_0 M_6) + \frac{Q_1}{R_1} &= 0 \\ \frac{\partial}{\partial x_1} (N_6 + c_0 M_6) + \frac{\partial N_2}{\partial x_2} + \frac{Q_2}{R_2} &= 0 \\ \frac{\partial Q_1}{\partial x_1} + \frac{\partial Q_2}{\partial x_2} - \left(\frac{N_1}{R_1} + \frac{N_2}{R_2} - q \right) + (u_3) &= 0 \\ \frac{\partial M_1}{\partial x_1} + \frac{\partial M_6}{\partial x_2} - Q_1 &= 0 \\ \frac{\partial M_6}{\partial x_1} + \frac{\partial M_2}{\partial x_2} - Q_2 &= 0 \end{aligned} \quad (8)$$

where

$$(u_3) = \frac{\partial}{\partial x_1} \left(N_1 \frac{\partial u_3}{\partial x_1} + N_6 \frac{\partial u_3}{\partial x_2} \right) + \frac{\partial}{\partial x_2} \left(N_6 \frac{\partial u_3}{\partial x_1} + N_2 \frac{\partial u_3}{\partial x_2} \right) \quad (9)$$

The resultants (N_i, M_i, Q_i) are related to (ϵ_i^0, κ_i) ($i, j = 1, 2, 6$) by

$$\begin{aligned} N_i &= A_{ij} \epsilon_j^0 + B_{ij} \kappa_j \\ M_i &= B_{ij} \epsilon_j^0 + D_{ij} \kappa_j \end{aligned} \quad (10)$$

$$\begin{aligned} Q_2 &= A_{44} \epsilon_4^0 + A_{45} \epsilon_5^0 \\ Q_1 &= A_{45} \epsilon_4^0 + A_{55} \epsilon_5^0 \end{aligned} \quad (11)$$

Here A_{ij} , B_{ij} and D_{ij} ($i, j = 1, 2, 6$) denote the extensional, flexural-extensional coupling, and flexural stiffnesses of the laminate:

$$(A_{ij}, B_{ij}, D_{ij}) = \sum_{k=1}^L \int_{\zeta_{k-1}}^{\zeta_k} Q_{ij}^{(k)} (1, \zeta, \zeta^2) d\zeta \quad (i, j = 1, 2, 6) \quad (12)$$

$$(A_{44}, A_{45}, A_{55}) = \sum_{k=1}^L \int_{\zeta_{k-1}}^{\zeta_k} (K_1^2 Q_{44}^{(k)}, K_1 K_2 Q_{45}^{(k)}, K_2^2 Q_{55}^{(k)}) d\zeta$$

The boundary conditions, derived from the virtual work statement, involve specifying either the essential boundary conditions (EBC) or the natural boundary conditions (NBC):

<u>EBC</u>	or	<u>NBC</u>
u_1		$N_1 n_1 + (N_6 - c_0 M_6) n_2$
u_2		$N_2 n_2 + (N_6 + c_0 M_6) n_2$
u_3		$\left\{ \begin{aligned} & (N_1 \frac{\partial u_3}{\partial x_1}) n_1 + (N_2 \frac{\partial u_3}{\partial x_2}) n_2 \\ & + (N_6 \frac{\partial u_3}{\partial x_2}) n_1 + (N_6 \frac{\partial u_3}{\partial x_1}) n_2 \\ & + Q_2 n_2 + Q_1 n_1 \end{aligned} \right.$
ϕ_1		$M_1 n_1 + M_6 n_2$
ϕ_2		$M_2 n_2 + M_6 n_1$ (13)

where (n_1, n_2) denote the direction cosines of the unit normal on the boundary of the midsurface of the shell.

The exact form of the spatial variation of the solution of Eqs. (8)-(13), for the small-displacement theory, can be obtained under the following conditions (see Reddy [27]):

- (i) Symmetric or antisymmetric cross-ply laminates: i.e., laminates with

$$A_{16} = A_{26} = B_{16} = B_{26} = D_{16} = D_{26} = A_{45} = 0. \quad (14)$$

- (ii) Freely supported boundary conditions:

$$N_1(0, x_2) = N_1(a, x_2) = M_1(0, x_2) = M_1(a, x_2) = 0$$

$$u_3(0, x_2) = u_3(a, x_2) = u_2(0, x_2) = u_2(a, x_2) = 0$$

$$\begin{aligned}
 N_2(x_1,0) &= N_2(x_1,b) = M_2(x_1,0) = M_2(x_1,b) = 0 \\
 u_3(x_1,0) &= u_3(x_1,b) = u_1(x_1,0) = u_1(x_1,b) = 0 \\
 \phi_2(0,x_2) &= \phi_2(a,x_2) = \phi_1(x_1,0) = \phi_1(x_1,b) = 0
 \end{aligned} \tag{15}$$

where a and b are the dimensions of the shell middle surface along the x_1 and x_2 axes, respectively. The time variation of the load does not influence the spatial form of the solution.

Note that the exact solution can be obtained only for cross-ply laminated shells with simply supported boundary conditions. For general lamination schemes, exact solutions are not available to date.

FINITE-ELEMENT MODEL

A typical finite element is a doubly-curved shell element in the x_1x_2 -surface. Over the typical shell element $\Omega^{(e)}$, the displacements $(u_1, u_2, u_3, \phi_1, \phi_2)$ are interpolated by expressions of the form,

$$\begin{aligned}
 u_i &= \sum_{j=1}^N u_i^j \psi_j(x_1, x_2) \quad , \quad i = 1, 2, 3 \\
 \phi_i &= \sum_{j=1}^N \phi_i^j \psi_j(x_1, x_2) \quad , \quad i = 1, 2
 \end{aligned} \tag{16}$$

where ψ_j are the interpolation functions, and u_i^j and ϕ_i^j are the nodal values of u_i and ϕ_i , respectively. For a linear isoparametric element ($N = 4$) this interpolation results in a stiffness matrix of order 20 by 20. For a nine-node quadratic element the element stiffness matrix is of order 45 by 45.

Substitution of Eq. (2) into the virtual work principle, Eq. (9) yields an element equation of the form

$$[K(\Delta)] = \{F\} \quad (17)$$

where $\{\Delta\} = \{\{u_1\}, \{u_2\}, \{u_3\}, \{\phi_1\}, \{\phi_2\}\}^T$, $[K]$ the element stiffness matrix, and $\{F\}$ is the force vector. In the interest of brevity, the coefficients of the stiffness matrices are included in Appendix I.

The element equations (17) can be assembled, boundary conditions can be imposed, and the resulting equations can be solved at each load step. Note that the stiffness matrix $[K]$ is a function of the unknown solution vector $\{\Delta\}$; therefore, an iterative solution procedure is required for each load step. In the present study, we used the direct iteration technique, which can be expressed as

$$[K(\{\Delta\}^r)]\{\Delta\}^{r+1} = \{F\} \quad (18)$$

where $\{\Delta\}^r$ denotes the solution vector obtained in the r -th iteration (at any given load step). At the beginning of the first load step, we assume that $\{\Delta\}^0 = \{0\}$ and obtain the linear solution at the end of the first iteration. The solution obtained at the end of the r -th iteration is used to compute the stiffness matrix for the $(r+1)$ -th iteration. At the end of each iteration (for any load step), the solutions obtained in two consecutive iterations are compared to see if they are close enough to terminate the iteration and to move on to the next load step. The following convergence criterion is used in the present study:

$$\left[\frac{\sum_{i=1}^N |\Delta_i^r - \Delta_i^{r+1}|^2}{\sum_{i=1}^N |\Delta_i^r|^2} \right]^{1/2} < 0.01 \quad (19)$$

where N is the total number of unknown generalized displacements in the finite element mesh.

To accelerate the convergence, a weighted average of the solution from last two iterations are used to compute the stiffness matrix:

$$[K\{\gamma\{\Delta\}^{r-1} + (1 - \gamma)\{\Delta\}^r\}]\{\Delta\}^{r+1} = \{F\} \quad (20)$$

where γ is the acceleration parameter, $0 < \gamma < 1$. In the present study a value of 0.25 - 0.35 was used.

NUMERICAL RESULTS

Here we present numerical results for some sample problems. To illustrate the accuracy of the present element, first few examples are taken from the literature on isotropic and orthotropic shells. Then results (i.e., deflections and stresses) for several laminated shell problems are presented. The results for laminated shells should serve as references for future investigations.

All of the results reported here were obtained using the double-precision arithmetic on an IBM 3081 processor. Most of the sample problems were analyzed using a 2 x 2 uniform mesh of the nine-node (quadratic) isoparametric rectangular element.

1. Bending of a simply supported plate strip (or, equivalently, a beam) under uniformly distributed load.

The problem is mathematically one-dimensional and an analytical solution of the problem, based on the classical theory, can be found in Timoshenko and Woinowsky-Krieger [28]. The plate length along the y-coordinate is assumed to be large compared to the width, and it is simply supported on edges parallel

to the y-axis. The following simply supported boundary conditions are assumed:

$$w = \psi_y = 0 \text{ along edges } x = 0, a. \quad (21)$$

All inplane displacement degrees of freedom are restrained. A 5 x 1 mesh of four-node rectangular elements in the half plate is used to analyze the problem. The data and results are presented in Fig. 2. The present result is in good agreement with the analytical solution.

2. Clamped square plate under uniform load.

Due to the biaxial symmetry, only one quadrant of the plate is modelled with the 2 x 2 mesh of nine-node elements (4 x 4 mesh of linear elements give almost the same result). Pertinent data and results are presented in Fig. 3 for side to thickness ratios $a/h = 10$ and 500. The result for $a/h = 500$ is in agreement with the results of Way [29]. The difference is attributed to the fact that the present model includes the inplane displacement degrees of freedom and transverse shear deformation.

Figure 4 contains transverse deflection versus load for clamped orthotropic, cross-ply, and angle-ply plates. The lamina properties are

$$E_1 = 25 \times 10^4 \text{ N/mm}^2, E_2 = 2 \times 10^4 \text{ N/mm}^2, G_{12} = G_{13} = 10^4 \text{ N/mm}^2$$

$$G_{23} = 0.4 \times 10^4 \text{ N/mm}^2, \nu_{12} = 0.25.$$

For the same total thickness the clamped orthotropic square plate is stiffer than both two-layer angle-ply and cross-ply plates.

3. Simply supported, isotropic spherical shell under point load.

The pertinent data of the shell is shown in Fig. 5. A uniform mesh of 2 by 2 quadratic elements is used in a quadrant. The effect of three types of simply supported conditions on the center deflection and center normal stress is investigated:

$$\begin{aligned}
 \text{SS-1: } & u = w = \psi_x = 0 \quad \text{at } y = b; \quad v = w = \psi_y = 0 \quad \text{at } x = a \\
 \text{SS-2: } & u = v = w = \psi_x = 0 \quad \text{at } y = b; \quad u = v = w = \psi_y = 0 \quad \text{at } x = a \\
 \text{SS-3: } & v = w = \psi_x = 0 \quad \text{at } y = b; \quad u = w = \psi_y = 0 \quad \text{at } x = a
 \end{aligned} \tag{22}$$

Table 1 contains the results for the three boundary conditions. It is clear from the results that all three boundary conditions give virtually the same results for $a/h = 160$, and differ significantly (especially SS-1 differs from both SS-2 and SS-3) for $a/h = 16$. Thus, the effect is more in thick shells than in thin shells. The stress σ_y shown in Fig. 5 is evaluated at point $x = y = 1.691$ " in the top layer

4. Simply supported isotropic cylindrical shell under point load.

The geometry and material properties of the shell are shown in Fig. 6. Once again, the effect of various simply supported boundary conditions (22) on the deflections and stresses for the problem is investigated using a uniform mesh of 2 x 2 quadratic elements. The results are presented in Table 2. For the geometry and loading used here ($R = 2540$, $a = 254$, $h = 12.7$), the boundary conditions have very significant effect on the solution. Boundary conditions SS-2 and SS-3 give almost the same results whereas SS-1 gives about 2 1/2 times the deflection given by SS-2 or SS-3 boundary conditions.

5. Clamped isotropic cylindrical shell under uniform loading.

Figure 7 contains the pertinent data and results for a clamped cylindrical shell (isotropic) subjected to uniform load. The results are compared with those obtained by Dhatt [30]. The agreement is very good.

6. Clamped orthotropic cylindrical shell subjected to internal pressure.

Figure 8 contains the geometry and plots of center deflection and center stress versus the internal pressure for the problem. The orthotropic material properties used in the present study are:

$$E_1 = 7.5 \times 10^6 \text{ psi}, E_2 = 2 \times 10^6 \text{ psi}, G_{12} = G_{13} = G_{23} = 1.25 \times 10^6 \text{ psi}$$

$$\nu_{12} = 0.25 \quad (23)$$

The present result, obtained using the 2 x 2 mesh of quadratic elements, is in excellent agreement with that obtained by Chang and Sawamiphakdi [31].

7. Nine-layer [0°/90°/0°.../0°] cross-ply spherical shell subjected to uniformly distributed load.

The following geometrical data is used in the analysis:

$$R_1 = R_2 = R = 1,000 \text{ in.}, a = b = 100 \text{ in.}, h = 1 \text{ in.} \quad (24)$$

Individual layers are assumed to be of equal thickness ($h_i = h/9$), with the zero-degree layers being the inner and outer layers. The following two sets of orthotropic-material constants, typical high modulus graphite epoxy material (the ratios are more pertinent here), for individual layers are used:

$$\text{Mat.-1: } E_1 = 25 \times 10^6 \text{ psi, } E_2 = 10^6 \text{ psi, } G_{12} = G_{13} = 0.5 \times 10^6 \text{ psi}$$

$$G_{23} = 0.2 \times 10^6 \text{ psi, } \nu_{12} = 0.25 \quad (25)$$

$$\text{Mat.-2: } E_1 = 40 \times 10^6 \text{ psi, } E_2 = 10^6 \text{ psi, } G_{12} = G_{13} = 0.6 \times 10^6 \text{ psi}$$

$$G_{23} = 0.5 \times 10^6 \text{ psi, } \nu_{12} = 0.25 \quad (26)$$

Figure 9 contains plots of center deflection (w/h) versus the load parameter ($\bar{P} = q_0 R^2 / E_2 h^2$) for the two materials. Shell constructed of Material 1 deflects more, for a given load, than the shell laminated of Material 2 (because Material 2 is stiffer), and consequently experiences greater degree of nonlinearity. Note that the difference between the nonlinear deflections of the two shells increase nonlinearly, indicating that the shell made of Material 2 can take much more (ultimate) load than apparent from the ratio of moduli of the two materials, $E_1^{(2)} / E_1^{(1)}$.

8. Effect of various simply-supported boundary conditions on the deflections of two-layer cross-ply spherical shells under uniform load.

As pointed out in Problems 3 and 4, the transverse deflection is sensitive to the boundary conditions on the inplane displacements of simply supported shells. To further illustrate this effect for laminated shells, a set of four types of boundary conditions are used, and the results are presented in Table 3. Here SS-4 has the following meaning:

$$\begin{aligned} \text{SS-4} \quad w = \psi_x = 0 \text{ on } x = 0 \text{ and } a \\ w = \psi_y = 0 \text{ on } y = 0 \text{ and } b \end{aligned} \quad (27)$$

Once again we note that SS-2 and SS-3 give almost the same deflections. Boundary conditions SS-1 and SS-4 give deflections an order of magnitude higher than those given by SS-2 and SS-3. Thus, boundary conditions SS-2 and SS-3 make the shell quite stiffer.

9. Two-layer cross-ply $[0^\circ/90^\circ]$ and angle-ply $[-45^\circ/45^\circ]$, simply-supported (SS-3) spherical shells.

Figure 10 contains the pertinent data and results (with different scales) for the cross-ply and angle-ply shells (of Material 2). It is interesting to note that the type of nonlinearity exhibited by the two shells is quite different; the cross-ply shell gets softer whereas the angle-ply shell gets stiffer with an increase in the applied load. While both shells have bending-stretching coupling due to the lamination scheme ($B_{22} = -B_{11}$ nonzero for the cross-ply shell and B_{16} and B_{26} are nonzero for the angle-ply shell), the angle-ply experiences shear coupling that stiffens the spherical shell relatively more than the normal coupling (note that, in general, shells get softer under externally applied inward load).

Figure 11 contains plots of center deflection, normal stress ($-\sigma_y$) and shear stress (σ_{yz}) at $x = y = 5.283$ " versus load for two-layer cross-ply ($0^\circ/90^\circ$) spherical shell (Material 1) under point load at the center of the shell. The nonlinearity exhibited by the stresses (especially σ_{yz}) is less compared to that exhibited by the transverse deflection.

10. Two-layer clamped cylindrical shells under uniform loads.

Figures 12 and 13 contain results (i.e., w , σ_y , σ_{xz} versus load) for cross-ply $[0^\circ/90^\circ]$ and angle-ply $[-45^\circ/45^\circ]$ clamped cylindrical shells under uniform load. The load-deflection curve for the cross-ply shell resembles that

of the isotropic shell in Fig. 7, but exhibits greater degree of nonlinearity (being stiffer). The angle-ply shell exhibits different type of nonlinearity (softening type) for all loads.

11. Quasi-isotropic, clamped, cylindrical shell under uniform load.

Two types of quasi-isotropic clamped cylindrical shells are analyzed:

$$\text{Type 1: } [0^\circ/45^\circ/90^\circ/-45^\circ]_{\text{sym.}} \quad (28)$$

$$\text{Type 2: } [0^\circ/\pm 45^\circ/90^\circ]_{\text{sym.}}$$

Material 1 properties are assumed for each lamina (8 layers). The geometric data and results are presented in Fig. 14. Compared to the results presented in Figs. 12 and 13, the quasi-isotropic shells have the 'near-inflection' point at higher loads; the load-deflection curve has essentially the same form as that of the cross-ply shell (see Fig. 12).

SUMMARY AND CONCLUSIONS

A shear-flexible finite element based on the shear deformation version of the Sanders' theory and the von Karman strains is developed, and its application to isotropic, orthotropic, and laminated (cross-ply and angle-ply) shells is illustrated via numerous sample problems. Many of the results, especially those of laminated shells, are not available in the literature and therefore should serve as references for future investigations. From the numerical computations it is observed that boundary conditions on the inplane displacements have significant effect on the shell deflections and stresses. Also, it is noted that the form of nonlinearities exhibited by different lamination

schemes (i.e., cross-ply and angle-ply) is different. It would be of considerable interest to verify these findings by experiments.

ACKNOWLEDGMENTS

The results reported here were obtained during investigations supported by Structural Mechanics Divisions of AFOSR and NASA-Lewis. The authors are grateful for the support.

Table 1. Effect of various simply supported boundary conditions on the center deflections and normal stress in spherical shells under point load ($E = 10^7$ psi, $\nu = 0.3$).

Load P/h^2	Solution	SS-1		SS-2		SS-3	
		$a/h=160$	$a/h=16$	$a/h=160$	$a/h=16$	$a/h=160$	$a/h=16$
4,000	$-w^*$	0.0155	-	0.0152	-	0.0152	-
	$-\sigma_x^*$	893	-	984	-	894	-
8,000	$-w^*$	0.0329	0.0349	0.0324	0.0255	0.0324	0.0258
	$-\sigma_x$	1,880	6,535	1,882	6,015	1,882	6,031
12,000	$-w^*$	0.0529	-	0.0522	-	0.0521	-
	$-\sigma_x$	2,980	-	2,985	-	2,986	-
16,000	$-w^*$	0.0760	0.0793	0.0752	0.0520	0.0751	0.0525
	$-\sigma_x$	4,220	13,230	4,228	12,200	4,229	12,240
20,000	$-w^*$	0.1038	-	0.1028	-	0.1027	-
	$-\sigma_x$	5,657	-	5,671	-	5,672	-
24,000	$-w^*$	0.1364	0.1083	0.1354	0.0792	0.1353	0.0800
	$-\sigma_x$	7,268	20,110	7,289	18,500	7,291	18,550
28,000	$-w^*$	0.1761	-	0.1752	-	0.1751	-
	$-\sigma_x$	9,128	-	9,160	-	9,162	-
32,000	$-w^*$	0.2234	0.1472	0.2227	0.1072	0.2227	0.1083
	$-\sigma_x$	11,180	27,170	11,220	24,930	11,230	25,000

* $w(0,0)$, $\sigma_x(A,A)$; $A = 1.691$

Table 2. Effect of various types of simply supported boundary conditions on the deflections and stresses of anisotropic cylindrical shell under point load.

Load, P (N)	$-w$ (mm)	SS-1 $-\sigma_y$ (N/mm ²)	$-w$	SS-2 $-\sigma_y$	$-w$	SS-3 $-\sigma_y$
250	2.5804(2)	2.868	0.6544(4)	1.706	0.6698(4)	1.706
500	5.1626(2)	5.713	1.3533(4)	3.478	1.3843(4)	3.477
750	7.7343(2)	8.506	2.1057(4)	5.327	2.1522(4)	5.321
1,000	10.278(2)	11.210	2.9234(4)	7.265	2.9855(4)	7.242
1,250	12.733(2)	13.80	3.8241(4)	9.312	3.9017(4)	9.288
1,500	15.204(2)	16.25	4.8349(4)	11.50	4.9279(4)	11.46
1,750	17.560(2)	18.560	6.0331(5)	13.91	6.1423(5)	13.85
2,000	19.843(2)	20.730	7.5316(6)	16.66	7.6610(6)	16.57

Table 3. Effect of various simply-supported boundary conditions on the transverse deflections of cross-ply $[0^\circ/90^\circ]$ spherical shells under uniform load.

q_0	SS-1	SS-2	SS-3	SS-4
0.50	0.3344	0.04246	0.04257	0.4592
0.75	0.5757	0.06599	0.06617	0.8255
1.00	0.9485	0.09144	0.09171	1.3845
1.25	1.6529	0.11926	0.11966	1.9589
1.50	2.2826	0.15008	0.15063	2.3597
1.75	2.6421	0.18478	0.18556	2.5951
2.00	2.8499	0.22473	0.22584	2.8074
2.25	3.0764	0.27425	0.27593	3.0284
2.50	3.2432	0.33534	0.33795	3.1948
2.75	3.4214	0.42970	0.43487	3.3719

REFERENCES

1. P. M. Naghdi, "A Survey of Recent Progress in the theory of Elastic Shells," Appl. Mech. Reviews, Vol. 9, No. 9, pp. 365-368, 1956.
2. C. W. Bert, "Analysis of Shells," Analysis and Performance of Composites, L. J. Broutman (ed.), Wiley, New York, pp. 207-258, 1980.
3. A. E. H. Love, "On the Small Free Vibrations and Deformations of the Elastic Shells," Phil. Trans. Roy. Soc. (London), Ser. A, Vol. 17, pp. 491-546, 1888.
4. E. Reissner, "A New Derivation of the Equations for the Deformation of Elastic Shells," Am. Jour. Math., Vol. 63, No. 1, pp. 177-184, 1941.
5. E. Reissner, "On Some Problems in Shell Theory," Structural Mechanics (Proceedings of the First Symposium on Naval Structural Mechanics), J. N. Goodier and N. J. Hoff (eds.), Pergamon Press, New York, pp. 74-114, 1960.
6. E. Reissner, "A Note on Generating Generalized Two-Dimensional Plate and Shell Theories," J. Appl. Math. Physics (ZAMP), Vol. 28, pp. 633-642, 1977.
7. J. L. Sanders, "An Improved First-Approximation Theory for Thin Shells," NASA Technical Report R-24, 1959.
8. S. A. Ambartsumyan, "Calculation of Laminated Anisotropic Shells," Izvestiia Akademiia Nauk Armenskoi SSR, Ser. Fiz. Mat. Est. Tekh. Nauk., Vol. 6, No. 3, p. 15, 1953.
9. S. A. Ambartsumyan, Theory of Anisotropic Shells, Moscow, 1961; English translation, NASA TT F-118, May 1964.
10. S. B. Dong, K. S. Pister, and R. L. Taylor, "On the Theory of Laminated Anisotropic Shells and Plates," Journal of Aerospace Sciences, Vol. 29, p. 969-975, 1962.
11. L. H. Donnell, "Stability of Thin Walled Tubes in Torsion," NACA Report 479, 1933.
12. G. E. O. Widera, and S. W. Chung, "A Theory for Non-Homogeneous Anisotropic Cylindrical Shells," Journal of Applied Mechanics (ZAMP), Vol. 21, pp. 378-399, 1970.
13. J. A. Zukas, and J. R. Vinson, "Laminated Transversely Isotropic Cylindrical Shells," Journal of Applied Mechanics, pp. 400-407, 1971.
14. S. B. Dong, and F. K. W. Tso, "On a Laminated Orthotropic Shell Theory Including Transverse Shear Deformation," Journal of Applied Mechanics, Vol. 39, pp. 1091-1097, 1972.

15. J. M. Whitney, and C. T. Sun, "A Refined Theory for Laminated Anisotropic, Cylindrical Shells," Journal of Applied Mechanics, Vol. 41, pp. 471-476, 1974.
16. G. E. O. Widera, and D. L. Logan, "Refined Theories for Nonhomogeneous Anisotropic Cylindrical Shells: Part I-Derivation," Journal of the Engineering Mechanics Division, Vol. 106, No. EM6, pp. 1053-1074, 1980.
17. D. L. Logan, and G. E. O. Widera, "Refined Theories for Nonhomogeneous Anisotropic Cylindrical Shells: Part II-Application," Journal of the Engineering Mechanics Division, Vol. 106, No. EM6, pp. 1075-1090, 1980.
18. L. A. Schmit, and G. R. Monforton, "Finite Element Analysis of Sandwich Plate and Laminate Shells with Laminated Faces," American Institute of Aeronautics and Astronautics Journal, Vol. 8, pp. 1454-1461, 1970.
19. S. C. Panda, and R. Natarajan, "Finite Element Analysis of Laminated Shells of Revolution," Computers and Structures, Vol. 6, pp. 61-64, 1976.
20. K. N. Shivakumar, and A. V. Krishna Murty, "a High Precision Ring Element for Vibrations of Laminated Shells," Journal of Sound and Vibration, Vol. 58, No. 3, pp. 311-318, 1978.
21. K. P. Rao, "A Rectangular Laminated Anisotropic Shallow Thin Shell Finite Element," Computer Methods in Applied Mechanics and Engineering, Vol. 15, 1978, pp. 13-33.
22. P. Siede, and P. H. H. Chang, "Finite Element Analysis of Laminated Plates and Shells," NASA CR-157106, 1978 (132 pages).
23. Y. S. Hsu, J. N. Reddy, and C. W. Bert, "Thermoelasticity of Circular Cylindrical Shells Laminated of Bimodulus Composite Materials," Journal of Thermal Stresses, Vol. 4, No. 2, pp. 115-177, 1981.
24. J. N. Reddy, "Bending of Laminated Anisotropic Shells by a Shear Deformable Finite Element," Fibre Science and Technology, Vol. 17, pp. 9-24, 1982.
25. A. Venkatesh and K. P. Rao, "A Doubly Curved Quadrilateral Finite Element for the Analysis of Laminated Anisotropic Thin Shells of Revolution," Computers and Structures, Vol. 12, pp. 825-832, 1980.
26. A. Venkatesh and K. P. Rao, "Analysis of Laminated Shells with Laminated Stiffeners Using Rectangular Shell Finite Elements," Computer Methods in Appl. Mech. Engng., Vol. 38, pp. 255-272, 1983.
27. J. N. Reddy, "Exact Solutions of Moderately Thick Laminated Shells," J. Engineering Mechanics, ASCE, to appear.
28. S. Timoshenko and S. Woinowsky-Krieger, Theory of Plates and Shells, 2nd ed., McGraw-Hill, New York, 1959.
29. S. Way, "Uniformly Loaded, Clamped, Rectangular Plates with Large Deformation," Proc. 5th Inter. Congr. of Appl. Mech., Cambridge, MA, 1938.

30. G. S. Dhatt, "Instability of Thin Shells by the Finite Element Method," IASS Symposium for Folded Plates and Prismatic Structures, Vienna, 1970.
31. T. Y. Chang and K. Sawamiphakdi, "Large Deformation Analysis of Laminated Shells by Finite Element Method," Computers and Structures, Vol. 13, pp. 331-340, 1981.

APPENDIX I

Stiffness Coefficients:

$$\text{Let } f_1 = \frac{1}{2} \frac{\partial u_3}{\partial x_1}, \quad f_2 = \frac{1}{2} \frac{\partial u_3}{\partial x_2}$$

$$\begin{aligned} [K^{11}] &= A_{11}[S^{11}] + A_{16}([S^{12}] + [S^{21}]) + A_{66}[S^{22}] \\ &\quad - c_0(B_{16}([S^{12}] + [S^{21}]) + 2B_{66}[S^{22}] - c_0 D_{66}[S^{22}]) + \frac{A_{55}}{R_1^2} [S^{00}] \end{aligned}$$

$$\begin{aligned} [K^{12}] &= A_{12}[S^{12}] + A_{16}[S^{11}] + A_{26}[S^{22}] + A_{66}[S^{21}] \\ &\quad - c_0(B_{26}[S^{22}] - B_{16}[S^{11}] + c_0 D_{66}[S^{21}]) + \frac{A_{45}}{R_1 R_2} [S^{00}] \end{aligned}$$

$$\begin{aligned} [K^{13}] &= f_1(A_{11}[S^{11}] + A_{16}[S^{12}] + [S^{21}]) + A_{66}[S^{22}] \\ &\quad + f_2 A_{12}[S^{12}] + A_{16}[S^{11}] + A_{26}[S^{22}] + A_{66}[S^{21}] \\ &\quad + \frac{1}{R_1} (A_{11}[S^{10}] + A_{16}[S^{20}]) + \frac{1}{R_2} (A_{12}[S^{10}] + A_{26}[S^{20}]) \\ &\quad - c_0 \left(\frac{B_{16}}{R_1} [S^{20}] + \frac{B_{26}}{R_2} [S^{20}] \right) - \frac{1}{R_1} (A_{45}[S^{02}] + A_{55}[S^{01}]) \\ &\quad - c_0 [f_1 (B_{16}[S^{21}] + B_{66}[S^{22}]) + f_2 (B_{26}[S^{22}] + B_{66}[S^{21}])] \end{aligned}$$

$$\begin{aligned} [K^{14}] &= B_{11}[S^{11}] + B_{16}[S^{12}] + [S^{21}] + B_{66}[S^{22}] \\ &\quad - c_0 (D_{16}[S^{21}] + D_{66}[S^{22}]) - \frac{1}{R_1} A_{55}[S^{00}] \end{aligned}$$

$$[K^{15}] = B_{12}[S^{12}] + B_{16}[S^{11}] + B_{26}[S^{22}] + B_{66}[S^{21}] \\ - c_0(D_{26}[S^{22}] + D_{66}[S^{21}]) - \frac{1}{R_1} A_{45}[S^{00}]$$

$$[K^{21}] = [K^{12}]^T$$

$$[K^{22}] = A_{22}[S^{22}] + A_{26}([S^{12}] + [S^{21}]) + A_{66}[S^{11}] + 2c_0 B_{66}[S^{11}] \\ + c_0(B_{26}([S^{12}] + [S^{21}]) + c_0 D_{66}[S^{11}]) - \frac{A_{44}}{R_2^2} [S^{00}]$$

$$[K^{23}] = f_1(A_{12}[S^{21}] + A_{26}[S^{22}] + A_{16}[S^{11}] + A_{66}[S^{12}]) \\ + f_2(A_{22}[S^{22}] + A_{26}([S^{21}] + [S^{12}]) + A_{66}[S^{11}]) \\ + \frac{1}{R_1} (A_{12}[S^{20}] + A_{16}[S^{10}]) + \frac{1}{R_2} (A_{22}[S^{20}] + A_{26}[S^{10}]) \\ + c_0 \left[\left(\frac{B_{16}}{R_1} + \frac{B_{26}}{R_2} \right) [S^{10}] \right] - \frac{1}{R_2} (A_{44}[S^{02}] + A_{45}[S^{01}]) \\ + c_0 [f_1(B_{16}[S^{11}] + B_{66}[S^{12}]) + f_2(B_{26}[S^{12}] + B_{66}[S^{11}])]]$$

$$[K^{24}] = B_{12}[S^{21}] + B_{26}[S^{22}] + B_{16}[S^{11}] + B_{66}[S^{12}] \\ + c_0(D_{16}[S^{11}] + D_{66}[S^{12}]) - \frac{1}{R_2} A_{45}[S^{00}]$$

$$[K^{25}] = B_{22}[S^{22}] + B_{26}([S^{21}] + [S^{12}]) + B_{66}[S^{11}] \\ + c_0(D_{26}[S^{12}] + D_{66}[S^{11}]) - \frac{1}{R_2} A_{44}[S^{00}]$$

$$[K^{31}]_{NL} = [2K^{13}]_{NL}^T, \quad NL = \text{Nonlinear portion of the matrix}$$

$$[K^{32}]_{NL} = [2K^{23}]_{NL}^T$$

$$\begin{aligned} [K^{33}] &= A_{45}[S^{12}] + A_{55}[S^{11}] + A_{44}[S^{22}] + A_{45}[S^{21}] \\ &+ 2[S^{11}](A_{11}f_1^2 + 2A_{16}f_1f_2 + A_{66}f_2^2) \\ &+ 2([S^{12}] + [S^{21}])(f_1^2A_{16} + (A_{12} + A_{66})f_1f_2 + f_2^2A_{26}) \\ &+ 2[S^{22}](A_{66}f_1^2 + 2A_{26}f_1f_2 + A_{22}f_2^2) \\ &+ [S^{00}]\left[\frac{1}{R_1}\left(\frac{A_{11}}{R_1} + \frac{A_{12}}{R_2}\right) + \frac{1}{R_2}\left(\frac{A_{12}}{R_1} + \frac{A_{22}}{R_2}\right)\right] \\ &+ ([S^{01}] + 2[S^{10}])(f_1\left(\frac{A_{11}}{R_1} + \frac{A_{12}}{R_2}\right) + f_2\left(\frac{A_{16}}{R_1} + \frac{A_{26}}{R_2}\right)) \\ &+ ([S^{02}] + 2[S^{20}])(f_1\left(\frac{A_{16}}{R_1} + \frac{A_{26}}{R_2}\right) + f_2\left(\frac{A_{12}}{R_1} + \frac{A_{22}}{R_2}\right)) \end{aligned}$$

$$\begin{aligned} [v^{34}]_j &= A_{55}[S^{10}] + A_{45}[S^{20}] \\ &+ 2f_1(B_{11}[S^{11}] + B_{16}([S^{12}] + [S^{21}]) + B_{66}[S^{22}]) \\ &+ 2f_2(B_{12}[S^{21}] + B_{66}[S^{12}] + B_{26}[S^{22}] + B_{16}[S^{11}]) \\ &+ \left(\frac{B_{11}}{R_1} + \frac{B_{12}}{R_2}\right)[S^{01}] + \left(\frac{B_{16}}{R_1} + \frac{B_{26}}{R_2}\right)[S^{02}] \end{aligned}$$

$$\begin{aligned}
[K^{35}] &= A_{45}[S^{10}] + A_{44}[S^{20}] \\
&+ 2f_1(B_{12}[S^{12}] + B_{66}[S^{21}] + B_{16}[S^{11}] + B_{26}[S^{22}]) \\
&+ 2f_2(B_{22}[S^{22}] + B_{26}([S^{12}]) + B_{26}[S^{21}]) + B_{66}[S^{11}] \\
&+ \left(-\frac{B_{16}}{R_1} + \frac{B_{26}}{R_2}\right)[S^{01}] + \left(-\frac{B_{12}}{R_1} + \frac{B_{22}}{R_2}\right)[S^{02}]
\end{aligned}$$

$$[K^{41}] = [K^{14}]^T, [K^{42}] = [K^{24}]^T, [K^{43}]_{NL} = \frac{1}{2} [K^{34}]_{NL}^T$$

$$[K^{44}] = D_{11}[S^{11}] + D_{16}([S^{12}] + [S^{21}]) + D_{66}[S^{22}] + A_{55}[S^{00}]$$

$$[K^{45}] = D_{12}[S^{12}] + D_{16}[S^{11}] + D_{26}[S^{22}] + D_{66}[S^{21}] + A_{45}[S^{00}]$$

$$[K^{51}] = [K^{15}]^T, [K^{52}] = [K^{25}]^T, [K^{53}]_{NL} = \frac{1}{2} [K^{35}]_{NL}^T$$

$$[K^{54}] = [K^{45}]^T$$

$$[K^{55}] = D_{22}[S^{22}] + D_{26}([S^{12}] + [S^{21}]) + D_{66}[S^{11}] + A_{44}[S^{00}]$$

$$[K^{\alpha\beta}]_{Linear} = [K^{\beta\alpha}]_{Linear}^T$$

where

$$S_{ij}^{\alpha\beta} = \int_{\Omega^e} \frac{\partial \psi_i}{\partial x_\alpha} \frac{\partial \psi_j}{\partial x_\beta} dx_1 dx_2, \quad S_{ij}^{00} = \int_{\Omega^e} \psi_i \psi_j dx_1 dx_2$$

It should be noted that although f_1 and f_2 are shown factored outside the matrices, in the evaluation of the coefficients by the Gauss quadrature f_1 and f_2 are considered as parts of the integrals. For example $f_1 A_{11} [S^{11}]$ is evaluated by

$$\int_{\Omega} f_1 A_{11} \psi_i \psi_j dx_1 dx_2 = \frac{1}{2} \sum_{I=1}^N \sum_{J=1}^N A_{11} \left[\left(\frac{\partial u_3}{\partial x_1} \right) \psi_i \psi_j \right]_{x_1=Z_I, x_2=Z_J} W_I W_J \det J_0$$

where N is the number of Gauss points, W_I and W_J are the Gauss weights, Z_I and Z_J are the Gauss points, and J_0 is the Jacobian of the transformation.

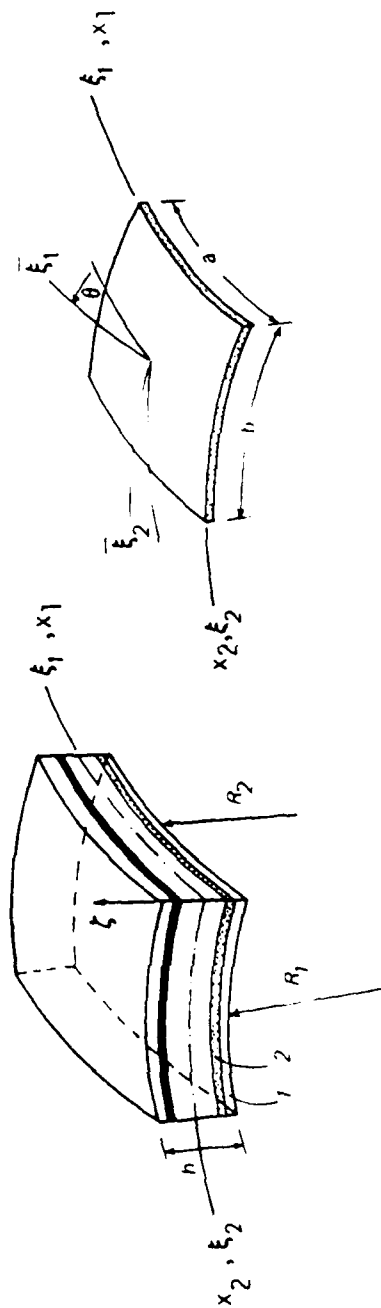


Figure 1 Geometry of a laminated, doubly-curved shell

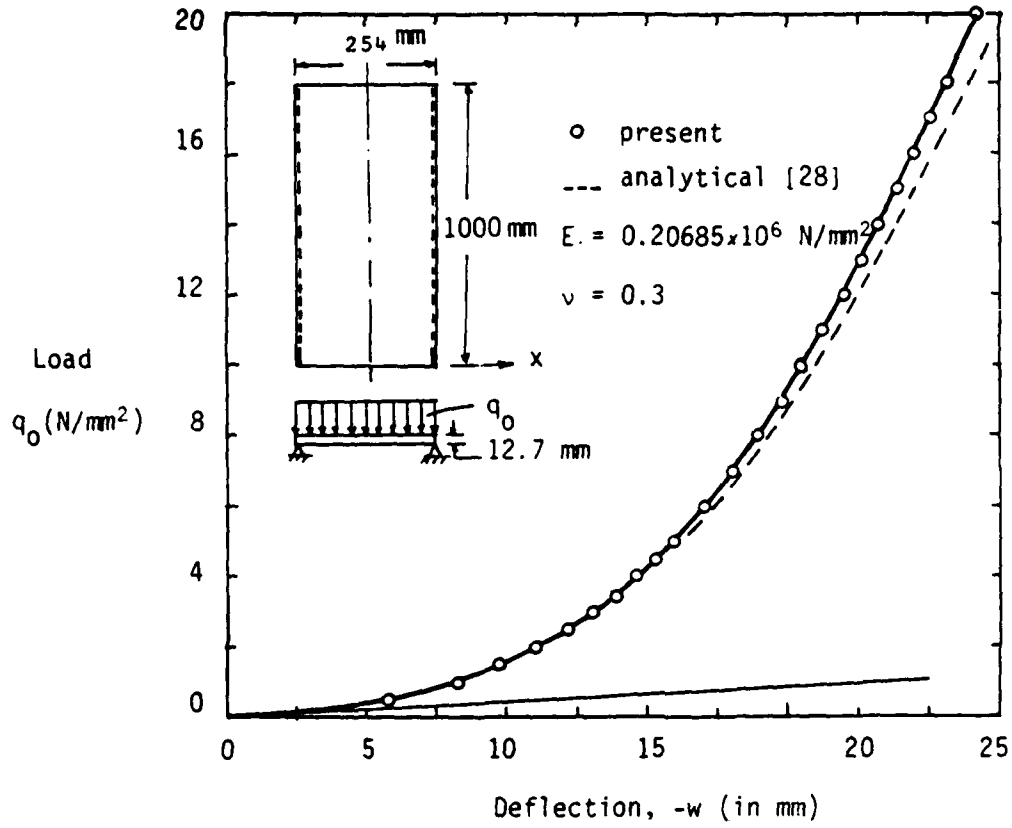


Figure 2. Bending of an isotropic simply supported plate strip under uniform load.

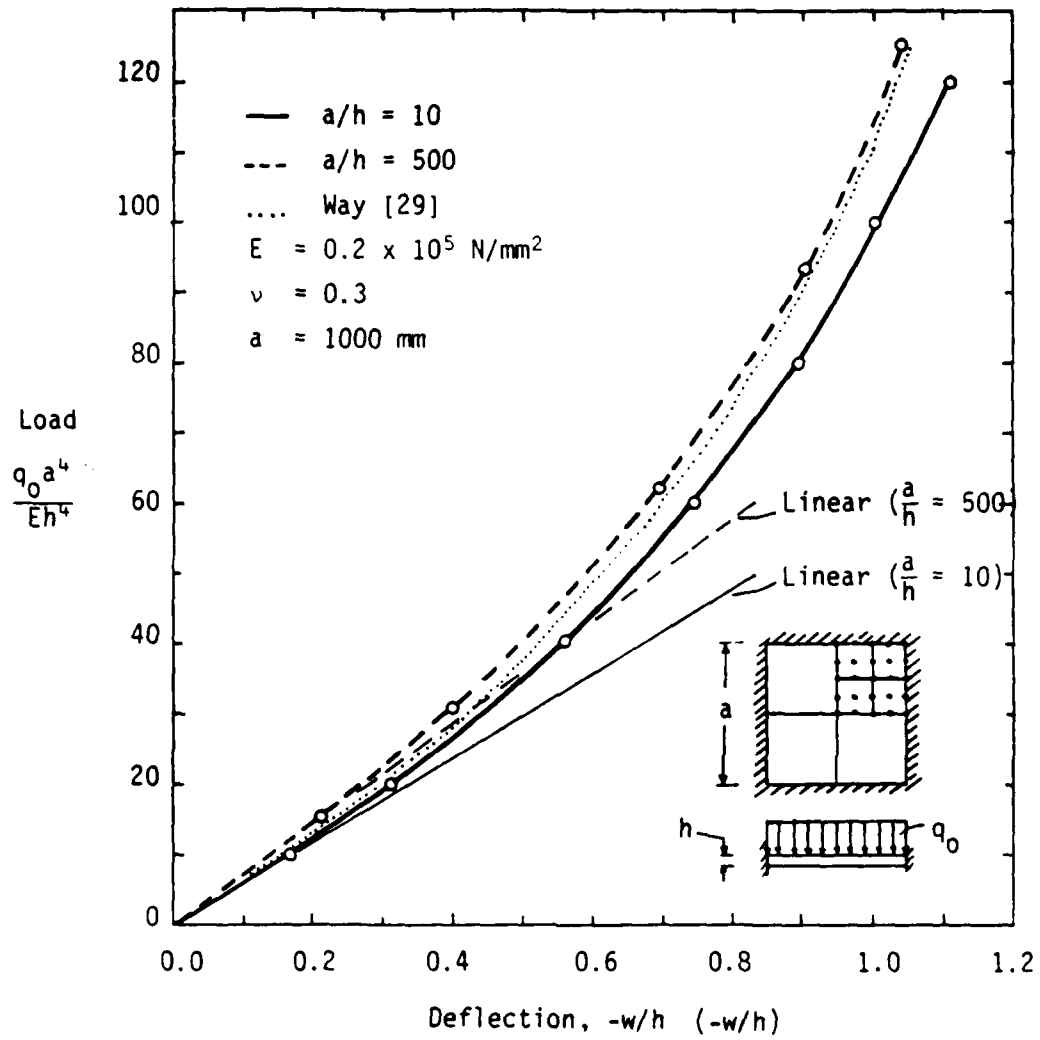


Figure 3. Bending of clamped isotropic square plate under uniform load.

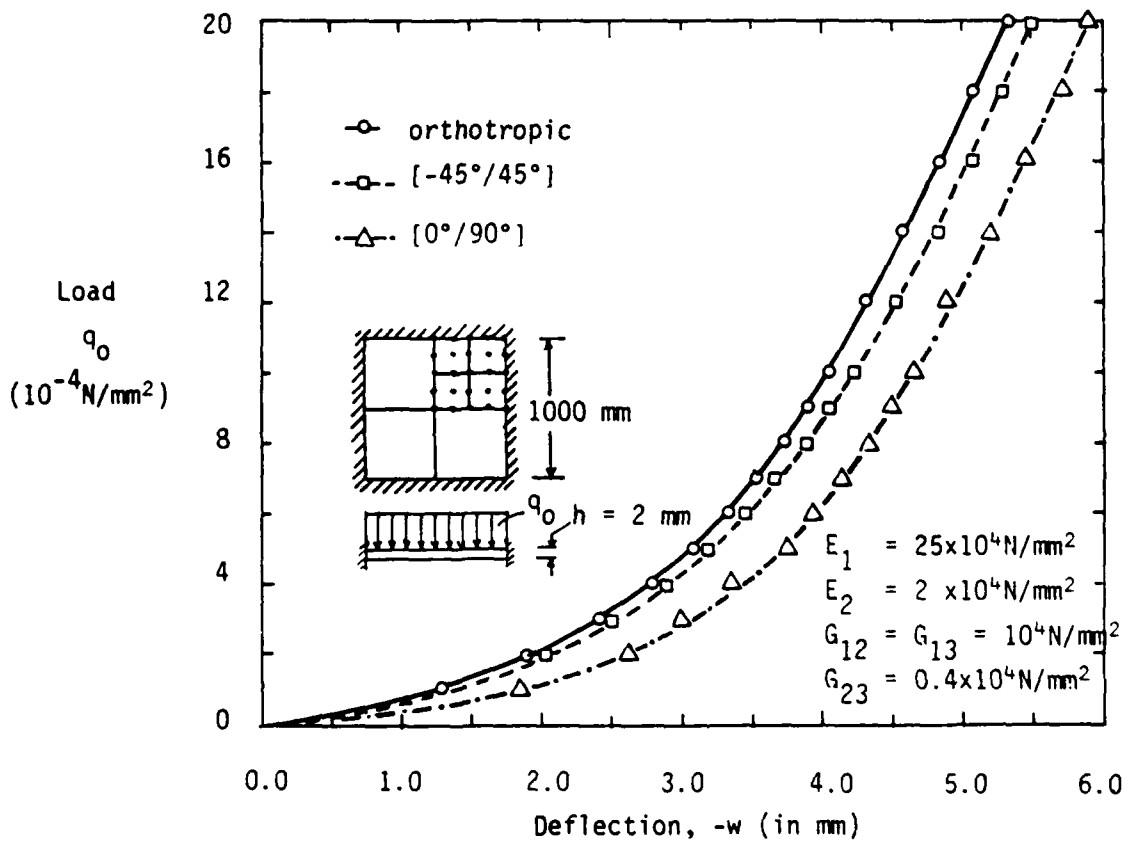


Figure 4. Bending of clamped orthotropic and laminated square plates under uniform load.

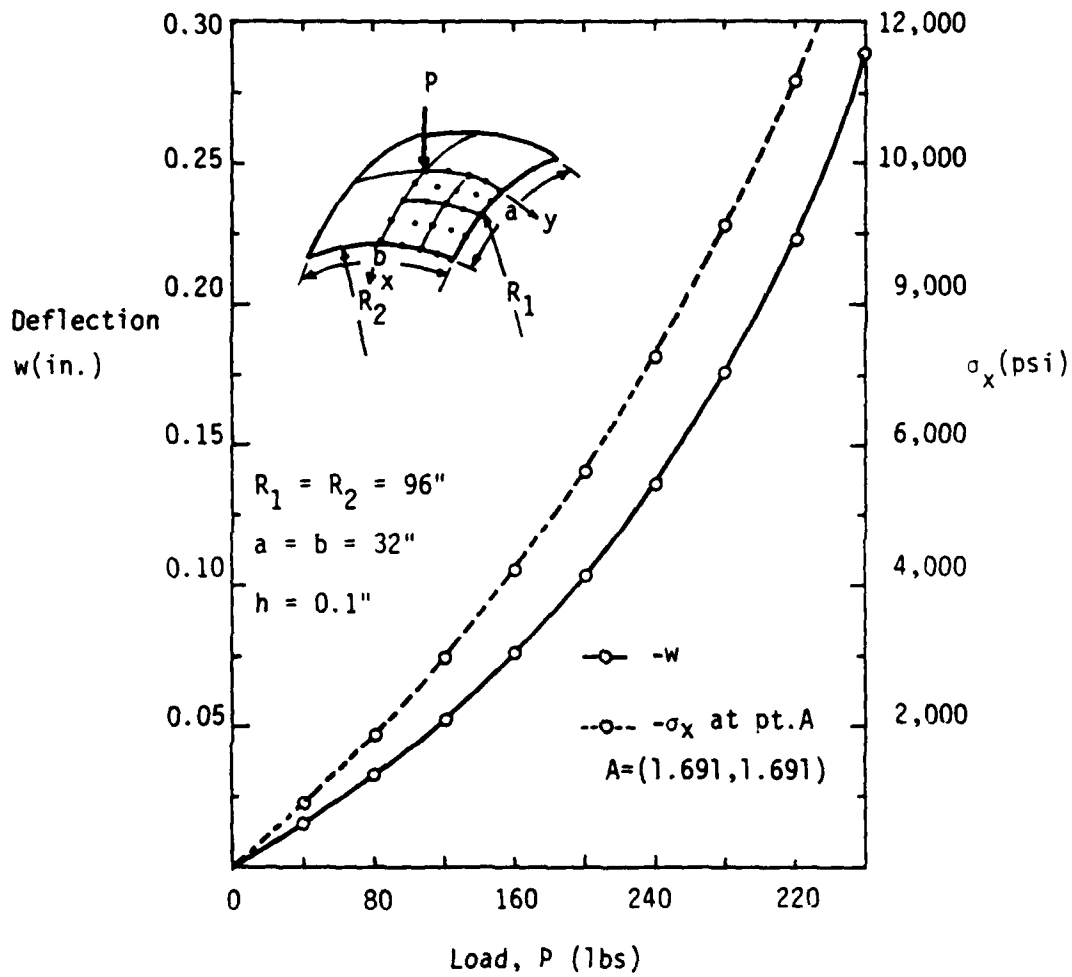


Figure 5. Bending of a simply supported (SS-3), isotropic, spherical shell under point load.

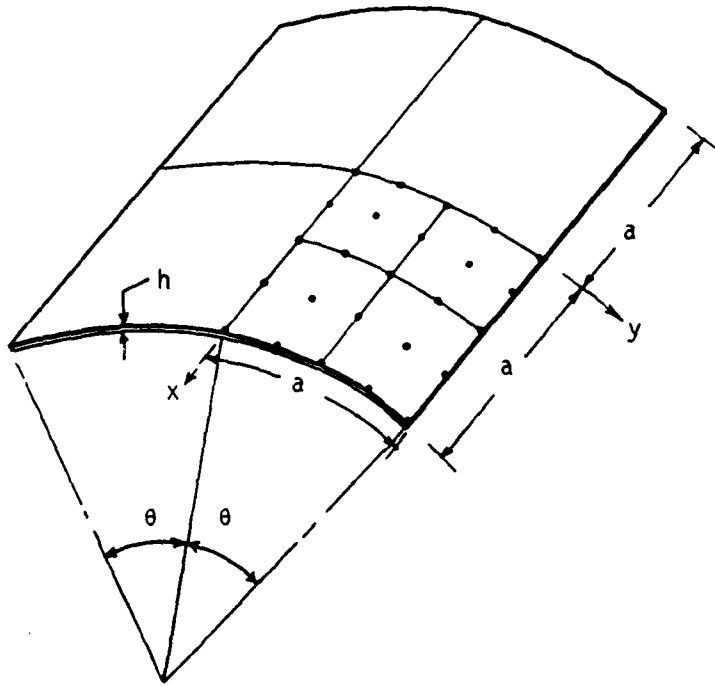


Figure 6. Geometry of a cylindrical shell.

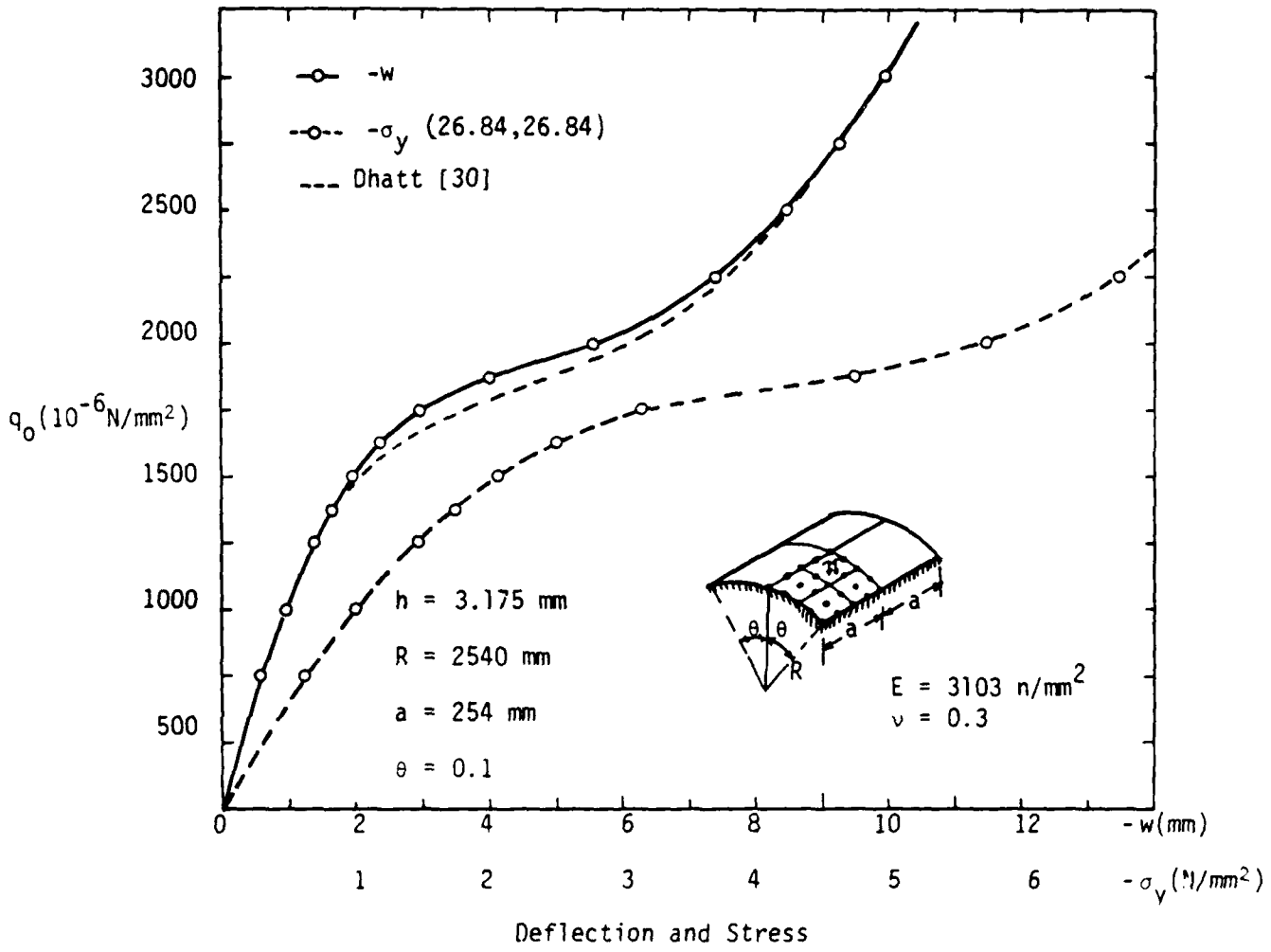


Figure 7. Bending of a clamped, isotropic, cylindrical shell under uniform load.

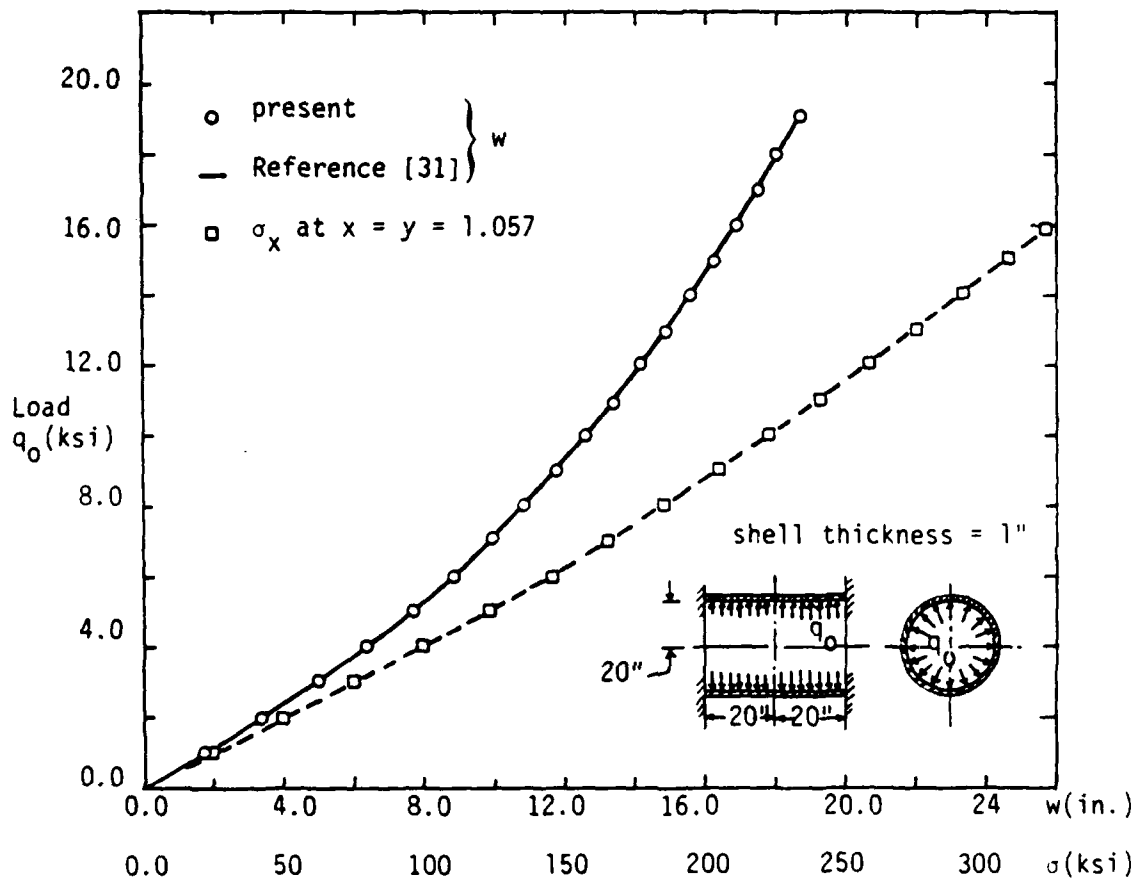


Figure 8. Bending of a clamped orthotropic cylindrical shell subjected to internal pressure.

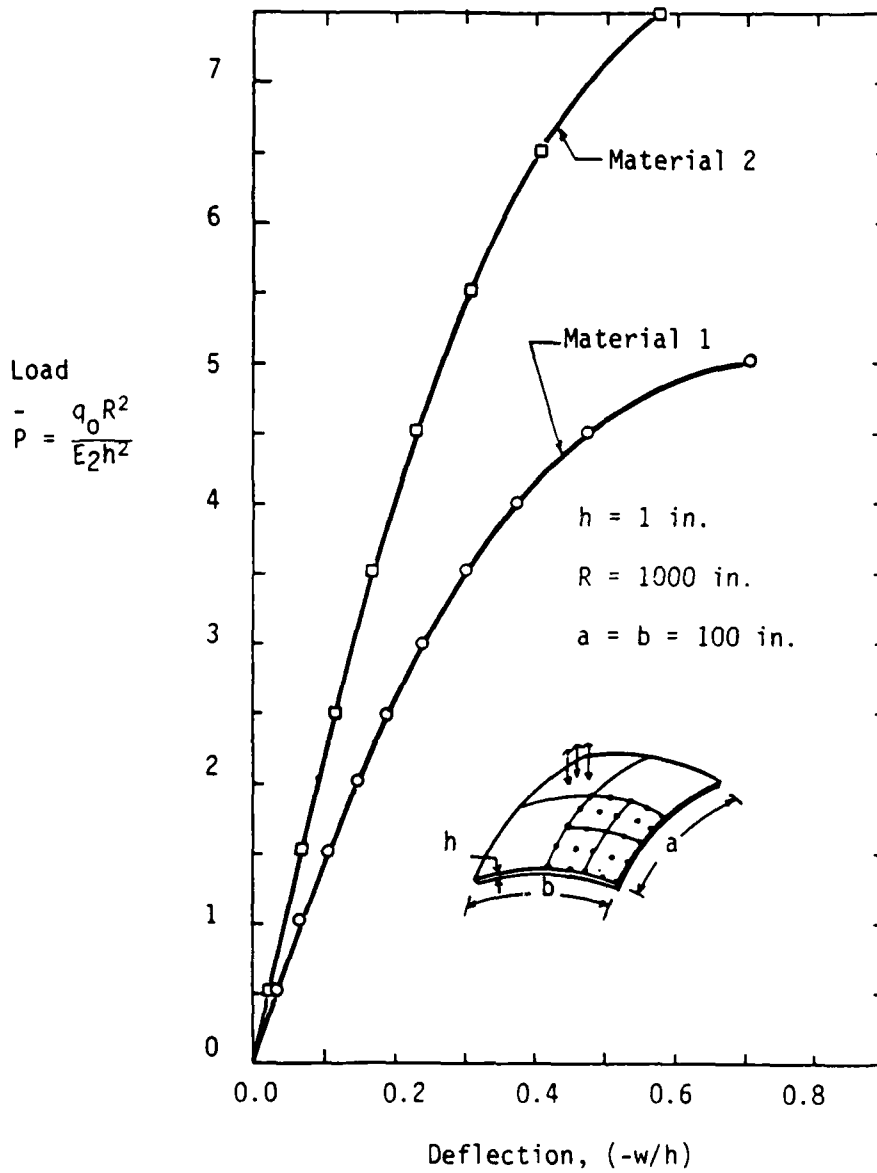


Figure 9. Bending of nine-layer cross-ply $[0^\circ/90^\circ/0^\circ/\dots]$ spherical shell subjected to uniformly distributed load.

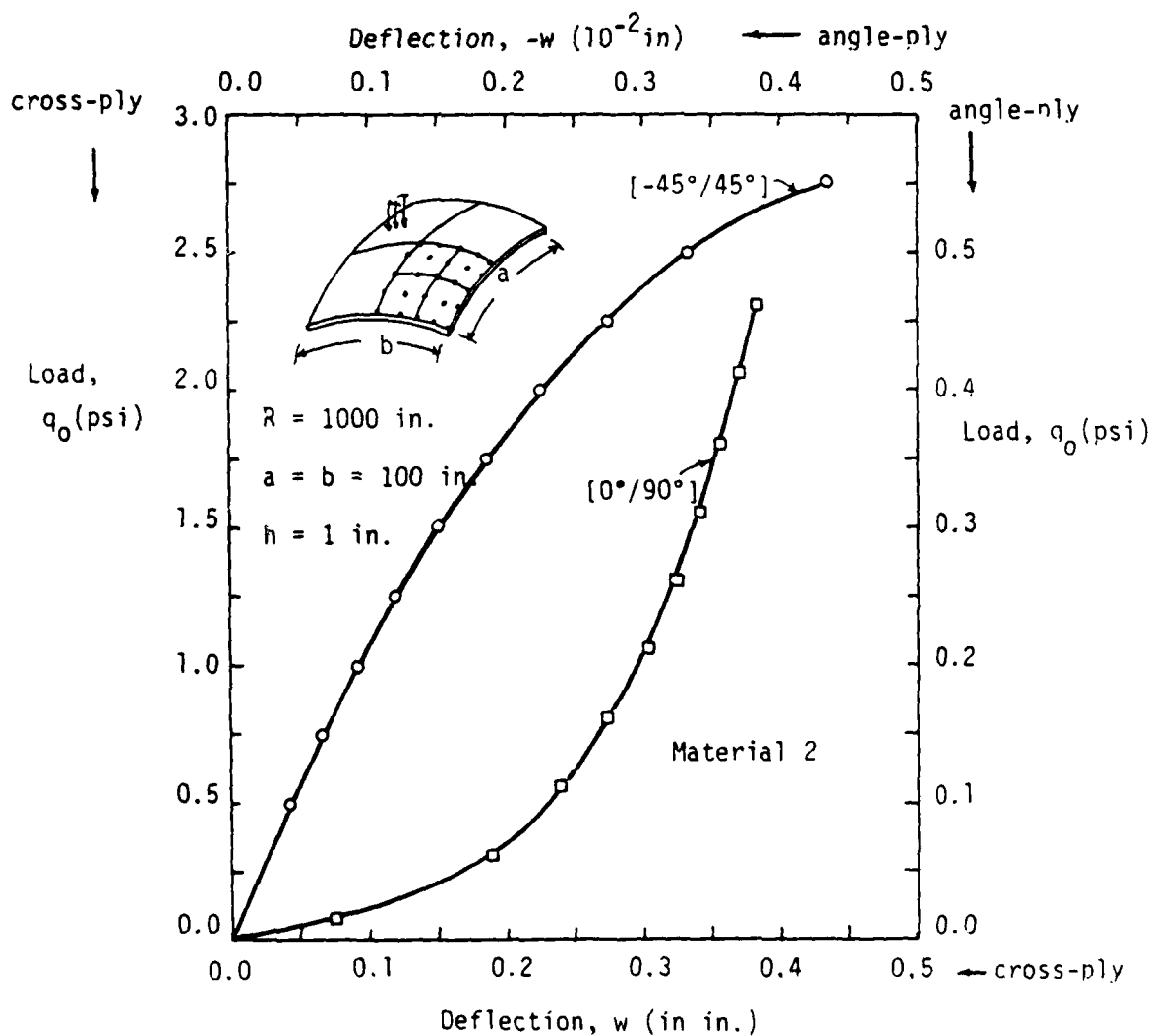


Figure 10. Bending of two-layer cross-ply and angle-ply, simply supported (SS-3) spherical shells under uniform load.

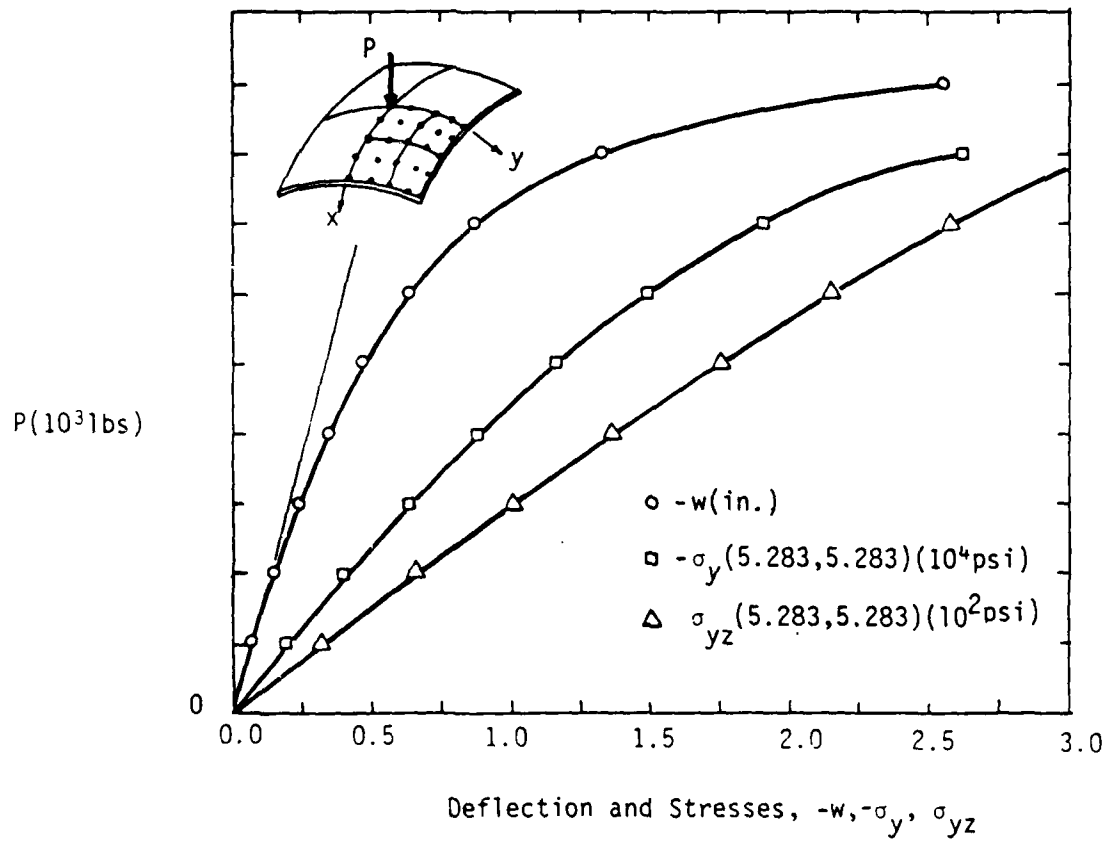


Figure 11. Bending of a cross-ply $[0^\circ/90^\circ]$ spherical shell (SS-3, Material 1), under point load.

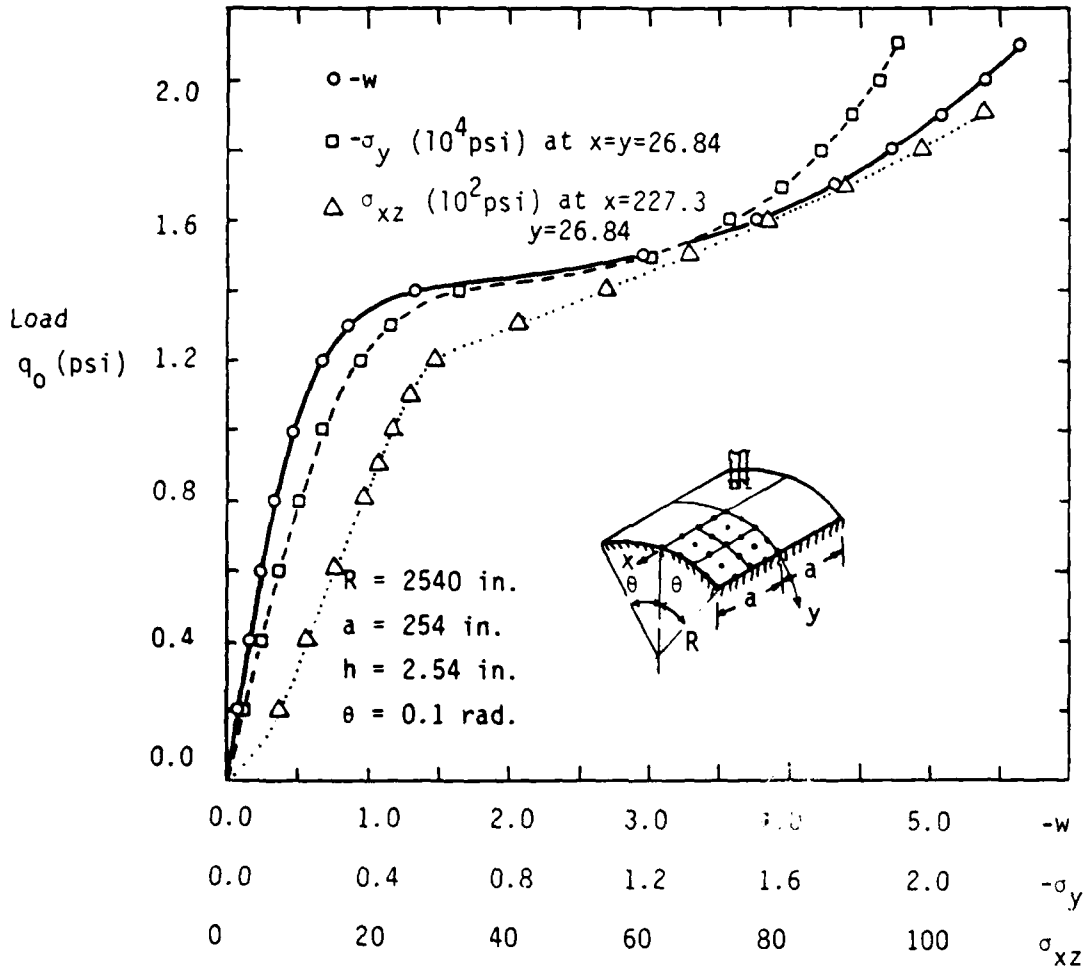


Figure 12. Bending of a clamped cross-ply $[0^\circ/90^\circ]$ cylindrical shell under uniform load.

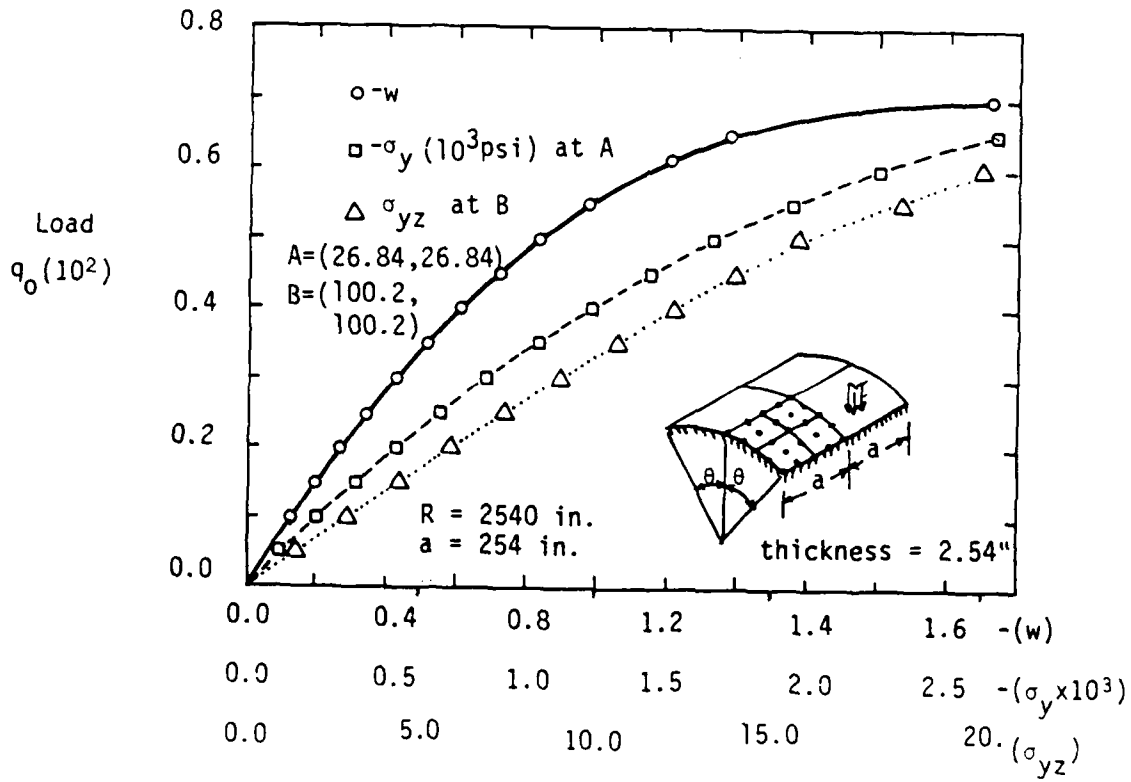


Figure 13. Bending of a clamped angle-ply [-45°/45°] cylindrical shell under uniform load.

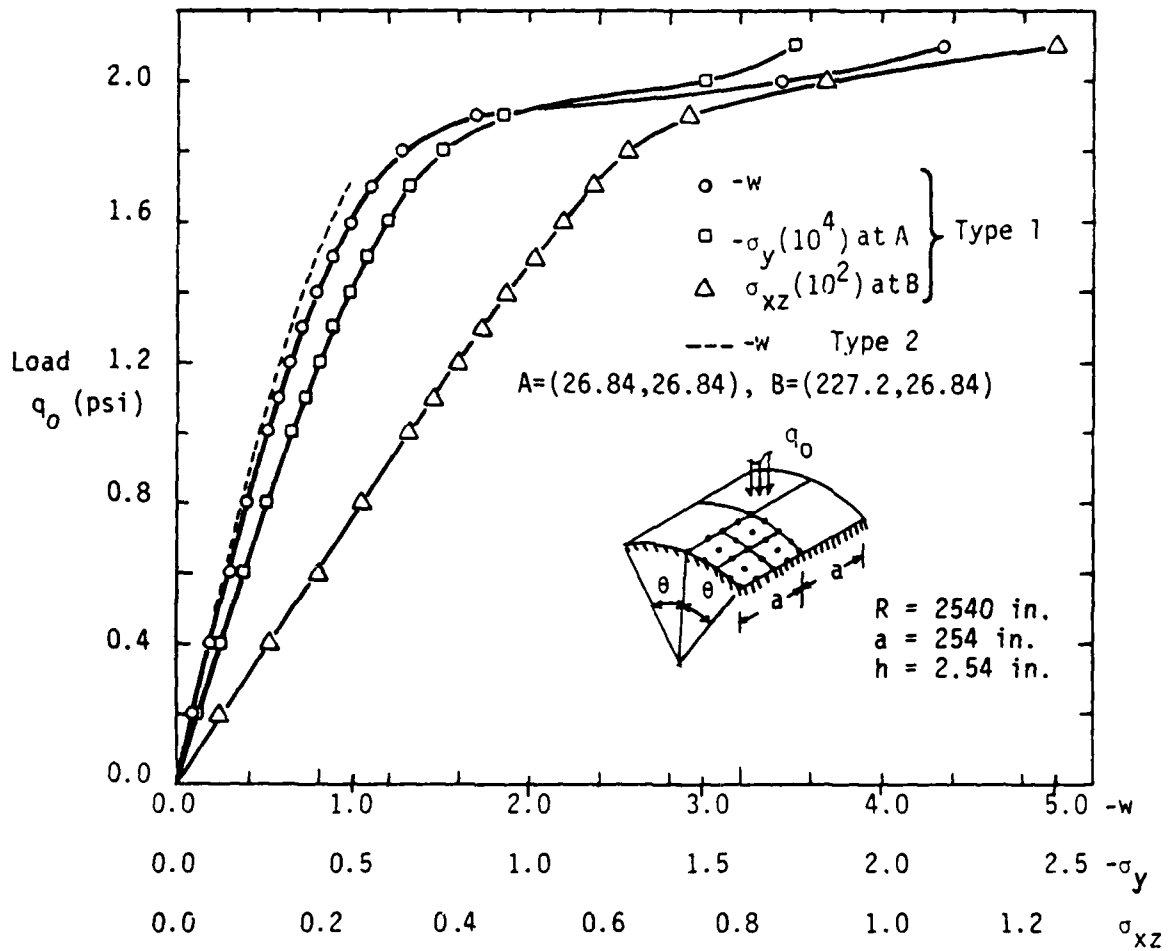


Figure 14. Bending of clamped quasi-isotropic cylindrical shells under uniform load.

UNCLASSIFIED

SECURITY CLASSIFICATION OF THIS PAGE (When Data Entered)

REPORT DOCUMENTATION PAGE		READ INSTRUCTIONS BEFORE COMPLETING FORM
1. REPORT NUMBER VPI-E-83.45	2. GOVT ACCESSION NO. AD-A135849	3. RECIPIENT'S CATALOG NUMBER
4. TITLE (and Subtitle) EXACT AND FINITE-ELEMENT ANALYSIS OF LAMINATED SHELLS		5. TYPE OF REPORT & PERIOD COVERED Interim
		6. PERFORMING ORG. REPORT NUMBER Tech. Report No. AFOSR-81-5
7. AUTHOR(s) J. N. Reddy		8. CONTRACT OR GRANT NUMBER(s) AFOSR-81-0142-B and C
		9. PERFORMING ORGANIZATION NAME AND ADDRESS Virginia Polytechnic Institute and State University Blacksburg, Virginia 24061
11. CONTROLLING OFFICE NAME AND ADDRESS United States Air Force Air Force Office of Scientific Research Bldg. 410, Bolling AFB, D.C.		10. PROGRAM ELEMENT, PROJECT, TASK AREA & WORK UNIT NUMBERS 2307/B1 (Structural Mechanics)
		12. REPORT DATE November, 1983
14. MONITORING AGENCY NAME & ADDRESS (if different from Controlling Office)		13. NUMBER OF PAGES 70
		15. SECURITY CLASS. (of this report) Unclassified
16. DISTRIBUTION STATEMENT (of this Report) This document has been approved for public release and sale; distribution unlimited.		15a. DECLASSIFICATION/DOWNGRADING SCHEDULE
17. DISTRIBUTION STATEMENT (of the abstract entered in Block 20, if different from Report)		
18. SUPPLEMENTARY NOTES The report has two parts. The first part deals with the exact solution of the linear theory governing shear deformable, doubly-curved laminated shells. The second part (coauthored with K.Chandrashekhara) deals with the finite-element analysis of the same theory but also includes the von Karman strains		
19. KEY WORDS (Continue on reverse side if necessary and identify by block number) Composite materials, exact solutions, finite element solutions, laminates, plates, shells, shear deformation theory, von Karman strains (geometric nonlinearity), vibration frequencies.		
20. ABSTRACT (Continue on reverse side if necessary and identify by block number) The two parts of the report deal with the exact solutions of the linear theory and finite-element analysis of the geometrically nonlinear (i.e. the von Karman theory of laminated, doubly-curved, shells, respectively. Numerical results are presented for both plates and shells. The results should serve as references for future investigations.		

DD FORM 1473

JAN 73

EDITION OF 1 NOV 55 IS OBSOLETE

UNCLASSIFIED

SECURITY CLASSIFICATION OF THIS PAGE (When Data Entered)

**DAT
ILM**